Article:

Pierre, M, Langone, A, Patacci, M orcid.org/0000-0003-1675-4643 et al. (1 more author) (2020) Towards a Southern European Tethyan Palaeomargin provenance signature: sandstone detrital modes and detrital zircon U–Pb age distribution of the Upper Cretaceous–Paleocene Monte Bignone Sandstones (Ligurian Alps, NW Italy). International Journal of Earth Sciences, 109 (1). pp. 201-220. ISSN 1437-3254

https://doi.org/10.1007/s00531-019-01797-5

Accepted for publication on International Journal of Earth Sciences

Towards a Southern European Tethyan Palaeomargin provenance signature: Sandstone detrital modes and detrital zircon U-Pb age distribution of the Upper Cretaceous–Paleocene Monte Bignone Sandstones (Ligurian Alps, NW Italy)

Pierre Mueller[1]*, Antonio Langone[2], Marco Patacci[3], Andrea Di Giulio[1]

[1]. Dipartimento di Scienze della Terra e dell'Ambiente, Universit‡ di Pavia, Pavia, Italy.

[2]. CNR ʻ Istituto di Geoscienze e Georisorse, Unita di Pavia, Via Ferrata 1, 27100 Pavia, Italy

[3]. Turbidites Research Group, School of Earth and Environment, University of Leeds, Leeds, LS2 9JT, UK.

Abstract

Constraining the source terranes of Alpine siliciclastic flysch sequences is crucial for building a clearer picture of the palaeogeography and geodynamic evolution of the Western Tethys in the framework of impending continental collision. This paper presents an integrated study that involves palaeocurrent dispersal analysis, sandstone petrography and detrital zircon geochronology of the Upper Cretaceous-Paleocene Monte Bignone Sandstones, a siliciclastic turbidite system deposited during the pre-collisional evolution of the Ligurian Alps. Palaeocurrent analysis illustrates an overall eastward transport of the proximal sediments in the present configuration. Considering the ca. 45-50° counter-clockwise rotation of the Tertiary Piedmont Basin and of the Corsica-Sardinia block in the late Paleogene, this indicates the derivation of the sediments from the northern margin of the Piedmont-Ligurian Ocean. Sandstone petrography records a stratigraphic evolution from quartzose sandstones towards lithic and then to lithic sub-arkosic composition. This trend is interpreted to reflect the gradual unroofing of the provenance terrane. The lithotypes of the recycled sedimentary rock fragments and the up-section increase in dolostone and carbonate clast proportions suggest the erosion of the sedimentary cover of the southern European palaeo-margin. New geochronological data (U-Pb detrital zircon ages) correspond to the pre-Alpine stages of crustal growth recorded in the Variscan Maures-Tanneron Massif, and therewith confirm the derivation of the sediments from the passive palaeo-European margin. This conclusion highlights the importance of the lower plate in providing the source of coarse-clastic deep-water successions during pre-collisional convergent steps. Results from this multi-proxy provenance analysis contribute to better defining the detrital signatures associated to the continental micro-fragments that constituted the palaeo-European plate as it supplied deep-sea siliciclastic sediments into the Piedmont-Ligurian ocean prior to continental collision.

1 Introduction

Orogenic belts originated from continent-continent collision are the result of vast displacements of the individual large-scale tectonic constituents (e.g. Dal Piaz 1999, Schmid et al. 2004; Handy et al. 2010). In the case of the Western Alps collisional zone, the understanding of the pre-collisional plate-tectonic configurations is crucial for assessing open questions regarding pre-orogenic geodynamics (Dal Piaz et al. 2003; Froitzheim et al. 2008; Molli 2008; Handy et al. 2010; Malusà et al. 2015). One classical approach to unriddle the Alpine puzzle is represented by the provenance analysis of pre- to syn-orogenic deep-water siliciclastic sedimentary sequences ("flysch" *sensu stricto* cf. Studer 1825; Homewood and Laveltin 1988) deposited in the subducted Piedmont-Ligurian ocean or along its thinned continental margins. These successions reflect sedimentation associated with the stages of the Alpine orogeny build-up since the onset of convergence in the early Late Cretaceous, when subduction of the European lithosphere beneath the Apulian plate initiated (e.g. Homewood 1983; Caron et al. 1989; Handy et al. 2010). Since siliciclastic successions record information about the nature of the source rocks and the uplift history of the provenance area, provenance constraints allow for palaeogeographic reconstructions of the source terranes, and aid in the regional-scale structural restoration of laterally displaced tectonic units (e.g. Dickinson et al. 1979; Valloni and Zuffa 1983; Zuffa 1985; Critelli et al. 2003; Shaw et al. 2014, among many others). Considering the complex build-up of the Alpine nappe stack, a steadily increasing number of studies show that the integration of petrographic, geochemical and geochronological analyses of pre- to syn-collisional turbiditic sandstones yield distinct detrital signatures which allow to uncover the geodynamic history of the closing oceanic basin and the bounding margins (e.g. Winkler 1984; Wildi 1985; Dunkl et al. 2001; Bracciali et al. 2007; Bütler et al. 2011; Chu et al. 2016; Lin et al. 2018; Carrapa et al. 2016; Di Giulio et al. 2017; Ragusa et al. 2017; Mueller et al. 2018). In light of the above, the linkage of detrital zircon U-Pb ages of sedimentary successions with the ages of rock-forming processes in candidate source areas allows for improved precision of provenance allocations (e.g. Fonneland et al. 2004; Dickinson and Gehrels 2009; Gehrels 2011; Thomas 2011).

Detritus derived from the bounding margins of the subducted Piedmont-Ligurian ocean has been categorized from many different perspectives such as sandstone modal composition (e.g. Winkler et al. 1984; Giorgis et al. 1999; Bütler et al. 2010; Ragusa et al. 2017), heavy mineral assemblages and geochemical signatures (Stanley 1965, Wildi 1985; Lihou and Mange-Rajetzky 1996; Thum et al. 2015), and U-Pb detrital zircon age patterns (e.g. Vezzoli et al. 2004; Bütler et al. 2010; Manzotti et al. 2015, 2016; Chu et al. 2016; Lin et al. 2018). Notably, recent studies, and essentially those aided by detrital zircon chronology, reveal that the "classic" Swiss flysch successions of the eastern Piedmont-Ligurian Ocean were dominantly sourced from the Adriatic plate (i.e. the Sesia extensional allochthon of continental crust; Bütler et al. 2011; Ragusa et al. 2017). With respect to "Alpine-vergent" subduction polarity (e.g. Stampfli et al 1998; Stampfli et al. 2002a; Handy et al. 2010), this indicates sedimentation in an active margin provenance scenario. By contrast, detrital zircon ages reported in several recent papers (e.g. Chu et al. 2016; Lin et al. 2018; Mueller et al. 2018) suggest that the re-activated passive margin of the lower plate (i.e. the external European continental units) provided the source of the Western Ligurian and Corsican flysches deposited in the western part of the Piedmont-Ligurian Ocean during the pre-collisional convergent steps.

We present further evidence for this hypothesis provided by the results of palaeocurrent analysis, sandstone petrography, and U-Pb detrital zircon chronology, applied to the siliciclastic Monte Bignone Sandstones ("Quarziti di Monte Bignone"; hereafter MBS) of the Borghetta d´Arroscia-Alassio Unit of the Western Ligurian Flysch complex. The results refine the characteristic petrographic and geochronological signature for the southernmost domain of the European Tethyan palaeo-margin.

2 Geological setting

2.1 Regional tectonic framework

The studied MBS form part of the Borghetto d'Arroscia-Alassio Unit of the Western Ligurian Helminthoid Flysch tectonic complex (WLF) in northern Italy (Fig. 1A-B). The WLF represents the structurally topmost part of the Upper Penninic Nappe pile, presently located on top of the Penninic basal thrust towards the Palaeo-European margin (e.g. Vanossi et al, 1986; Di Giulio 1992; Seno et al. 2005; Maino et al. 2015). It is composed of units formed by the deep-marine cover of the Piedmont-Ligurian ocean off-scraped from their substratum and incorporated in the Upper Cretaceous-Palaeogene accretionary prism along the Ligurian Alps transect of the Alpine subduction system (Lanteaume 1962; Vanossi et al. 1986; Di Giulio 1992; Marroni and Pandolfi, 2010). The main tectonic units are: the San Remo-Monte Saccarello Unit, the Moglio-Testico Unit, the Borghetto Unit and the Colla Domenica-Leverone Unit. They contain two prominent coarse-grained siliciclastic deep-water systems within dominant Helminthoid-type calcareous-marly flysches: the Bordighera Sandstones in the San Remo-Monte Saccarello Unit (Mueller et al. 2018 and references therein), and the Monte Bignone Sandstones in the Borghetto d´Arroscia-Alassio Unit (Galbiati, 1986; Fig. 1B). The present configuration of the tectonic units, with the oldest unit resting on top of the nappe pile (Fig. 1C), documents the tectonic inversion pattern characteristic of accretionary prisms (Di Giulio, 1992).

The Borghetto d'Arroscia-Alassio Unit experienced multiple ductile-brittle deformation phases (Galbiati, 1986). The initial phase was characterized by the development of S-verging recumbent folds and thrust planes that record the S-vergent tectonic phase which also generated the contacts between individual flysch units. The second phase is typified by opposite, N-vergent, more open, locally faulted folds. A third large-scale S-verging deformation phase resulted in the overall westward inversion of the geometric relations between the flysch units.

Borghetto d´Arroscia-Alassio Unit

Stratigraphically, the Borghetto d´Arroscia-Alassio Unit is inferred to span from the lower Senonian into the Paleocene-Eocene (Lanteaume 1962; Di Giulio 1985). It has been subdivided into three formations (Fig. 1C) which are separated by stratigraphic contacts (e.g. Boni and Vanossi 1960, 1972; Galbiati 1982; Marini and Terranova 1985). From base to top they are: (i) the Ranzo Shales ("Peliti di Ranzo"), (ii) the Monte Bignone Sandstones ("Quarziti di Monte Bignone"), and (iii) the Ubaga Limestones ("Calcari di Ubaga"). Owing to the scarcity and poor preservation of microfaunal assemblages, the biostratigraphic placement of the siliciclastic members remains vague (cf. Marini and Terranova 1985). Only the topmost formation, the Ubaga Limestones, can be certainly assigned to a Paleocene-Eocene depositional age (Di Giulio 1985).

The Ranzo Shales represent the so called "basal complex" of the Borghetto d´Arroscia-Alassio Unit (Galbiati 1986; Marini and Terrannova 1985; Di Giulio 1992). It is made up of a monotonous succession of dark shales, with sporadic intercalations of thin-bedded calcareous turbidites and of fine-grained siliciclastic turbiditic beds. Due to the decollement from their original substratum and pervasive deformations, the maximum thickness of the formation is unknown; however, the maximum outcropping thickness is in the range of 50 m (Marini and Terranova 1985; Galbiati 1986).

The Monte Bignone Sandstones (MBS) comprise greyish to whitish-reddish, medium- to thick-bedded quartzarenites. They reach an estimated maximum thickness of ca. 230 m (Galbiati 1986), and are subdivided into four members. Two main quartzarenitic units (Lower and Upper Quartzites units; Fig. 2 A-B; Fig. 3 A-B) at their bases interdigitate with polymictic coarse-grained conglomeratic intervals ("Lower" and "Middle" conglomerates). The quartzarenitic units are characterized by good down-current continuity, whereas the conglomeratic intervals rapidly become replaced by pelitic intervals ("Lower" and "Middle" shales of Galbiati 1986;) towards the more distal domain (see also Fig. 2 A-B). Within the pelitic members, chaotic bodies with exotic clasts (basalt breccias, radiolarian cherts and limestone debris) are locally present (Fig. 3C). They have been interpreted as debris-flow deposits which document seafloor remobilisation related to mud-diapirism in front of the accretionary prism (Di Giulio 1992).

The Ubaga Limestones are a rhythmic succession of medium- to very thick-bedded calcareous turbidites belonging to the wide family of the Alpine Helminthoid Flysches (e.g. Caron et al. 1989; Di Giulio 1992). The typical facies motif is that of beds with thin, silty bed bases (siliciclastic or mixed siliciclastic and calcareous) and thick calcareous or marly mudstone caps. They are separated from the MBS by a transitional lithozone characterized by alternations of thin-bedded, fine-grained siliciclastic and calcareous turbidites ("San Pantaleo lithozone"; Fig. 2A-B). The bases of the calcareous turbidites locally display ichnofossils of the typical *Helminthoides* flysch association (Boni and Vanossi 1972).

Based on qualitative analysis of the clast lithologies of the proximal conglomerates, several authors proposed a provenance of the sediment forming the Borghetto d´Arroscia-Alassio Unit from the Briançonnais terrane and the Pre-Piedmont domain (e.g. Galbiati 1982; Marini and Terranova 1985; Vanossi et al. 1986), the domain that represents the distalmost part of the hyperextended European continental margin (e.g. Decarlis et al. 2017).

3 Methodology

Two stratigraphic sections that offer continuous exposures of the two coarse-grained units of the MBS (Lower and the Upper Quarzites units) were chosen for this study (Figs. 1C and 2C-D). Detailed sedimentological logging (drawn in the field at 1:25 scale) was undertaken with the aid of a high-precision Jacob's staff (Patacci, 2016). Palaeocurrent directions were determined by the measurement of the orientations of turbidite bed sole markings (flute and groove casts) and of the dip direction of ripple laminae and cross-bed lee slopes. Thirty sandstone samples were selected for thin section preparation (Fig. 2). The bulk of samples (27) were collected in the most proximal outcrop "Capo Santa Croce" near the town of Alassio (GPS 44.0158, 8.1929; all coordinates are in WGS84). Three samples were acquired in the more distal part of the system, from a roadcut section between the towns of Canata di Ranzo and Ubaghetta (GPS 44.0556, 8.0005). Two additional sandstone samples were collected at the distal section for U-Pb detrital zircon geochronology.

Petrographic analysis was conducted by point-counting a minimum of 200 grains under the optical microscope, following the approach proposed in the guidelines of Di Giulio and Valloni (1992). In order to reduce compositional bias due to grain size effects, the Gazzi-Dickinson approach was utilized (Gazzi 1960; Dickinson 1970; Ingersoll et al. 1984). Recalculations of the framework grain modal proportions were performed according to the scheme of Dickinson et al. (1979). Detrital zircons were separated by conventional techniques (heavy liquid and magnetic separation) from two ca. 2 kg medium- to fine-grained sandstone samples. Only one sample (QdMZ_1) yielded a sufficient number of zircon grains for further analysis. Zircons were handpicked from the heavy mineral fraction, placed into epoxy resin mounts and polished to expose the zircon cores. Prior to U-Pb radiometric dating, the internal structure of detrital zircons was imaged using cathodoluminescence. LAM-ICP-MS analyses on detrital zircons were conducted utilizing the system configuration and methodology reported in Perotti et al. (2017) at the CNR laboratory at the University of Pavia. Details on the analytical setup are presented in the supplementary data file. Zircon grains were commonly analysed at one spot in the grain cores. In the cases of overgrowth rims greater than 25 microns, rims were also analysed. Mass bias and laser-induced fractionation were corrected by adopting external standards, utilizing the GJ-1 zircon as primary reference material (608.5 ± 0.4 Ma; Jackson et al. 2004). For means of quality control the unknown detrital zircons were bracketed by reference zircons 91500 (1065.4 ± 0.6 Ma; Wiedenbeck et al. 1995) and Plešovice (337.1 ± 0.4 Ma; Slama et al. 2008). Data reduction was carried out with the *GLITTER* software package (van Achterbergh et al. 2001). Detrital zircon U-Pb data with discordance >10% were discarded. Reported ages were calculated on the basis of $^{206}Pb/^{238}U$ ratios for grains younger than 1400 Ma and $^{206}Pb/^{207}Pb$ data for older grains (Gehrels et al. 2009). Detrital zircon age distributions were illustrated as probability density plots (PDPs) using the DensityPlotter 8.1 software (Vermeesch 2012). Cumulative density functions (CDFs) and a multidimensional scaling (MDS) map (Vermeesch 2013) were plotted utilizing the IsoplotR software (Vermeesch 2018).

4 Results

4.1 Sedimentary facies and palaeocurrents

The proximal "Capo Santa Croce" outcrop displays an overall coarsening-upward and thickening-upward trend delineated by the up-section transition from thin- to medium-bedded (outcrop-scale) tabular sandstones into thick-bedded lenticular coarse sandstones and pebbly conglomerates (Fig. 2C). The conglomerates are typically clast-supported. Scoured contacts between individual conglomeratic beds and bed-sets are common. The distal Ubaghetta section features multiple packages of medium- to thick-bedded sandstones that alternate with intervals dominated by mudstones and fine-grained thin-bedded sandstones (Fig. 2D). The sandstones are normally graded and do not exceed coarse sand grain size. Locally, the sandstones exhibit planar and wavy stratification. Towards their tops they sporadically display ripple laminations. Beds are non-amalgamated. They have sharp bases and sharp to gradational tops, and they exhibit tabular geometries at the outcrop scale (10s of metres). In the proximal outcrop, the transition from tabular strata into very coarse-grained conglomerate lenses is interpreted as reflecting the progradation of a proximal canyon into a channel-mouth depositional environment, most probably located at the break of slope of the continental margin (e.g. Lopez Jimenez et al. 2018). By contrast, the outcrop-scale tabular bed geometries, the characteristic alternations between sand-rich and heterolithic packages recorded in the distal outcrop together with the non-erosive nature and the arrangement of sedimentary structures that typify the Ubaghetta section is regarded as representative of a poorly confined to unconfined lobe environment (e.g. Marini et al. 2015).

Palaeocurrent analysis from the proximal section yielded 51 indicators of sediment dispersal orientation (two from groove casts, one from a flute cast and 48 from cross-strata foresets). 15 measurements were acquired from the more distal Ubaghetta section (six groove casts, six flute casts and three from ripple foresets). The proximal outcrop displays a relatively tight easterly sediment transport direction, whereas the more distal outcrop shows a more dispersed, overall northerly sediment dispersal (see palaeocurrent roses in Figs. 2 C&D). In view of the late Paleogene ca. 45-50° counter-clockwise rotation of the Tertiary Piedmont Basin and the Corsica-Sardinia Block (cf. Maffione et al. 2008 and references therein), we interpret the east-ward sediment dispersal recorded in the proximal outcrop as providing evidence of a source terrane located at the northern to northwestern margin of the Piedmont-Ligurian Ocean (with flows dispersing toward SE). Considering the inferred less confined distal depositional environment, we interpret the palaeocurrent recorded in the distal Ubaghetta section as indicating deposition of the sandstone lobes along the basin axis, presumably parallel to the base-of-slope.

4.2 Sandstone Petrography

Thin sections from the Monte Bignone Sandstones indicate highly compacted, moderately well-sorted to relatively poorly sorted sandstones (Fig. 4). Framework grains are typically sub-angular to rounded. Primary categories of framework grains comprise quartz, feldspar (potassium feldspar and plagioclase) and lithic fragments. Samples generally contain high proportions of quartz, very low to low proportions of feldspar, and variable (low to moderate) proportions of lithic fragments ($Qt_{51\text{-}96}F_{1\text{-}19}L1_{1\text{-}31}$; mean $Qt_{83}F_5L_{12}$). Quartz occurs in both mono- and polycrystalline varieties as typically sub-angular to sub-rounded grains (Fig. 4A-B). K-feldspar (dominantly orthoclase and microcline; see Fig. 4C) is typically more abundant than plagioclase. The lithic group is dominated by a variety of sedimentary (Fig.4C) and volcanic fragments (Fig. 4D). Plutonic and low-grade metamorphic fragments (Fig. 4C-E) are also common, albeit their shares vary significantly up-section. Among the sedimentary fragments, carbonate clasts (Fig. 4F), represented by both micritic limestone (Fig. 4G-J) and dolostone (Fig. 4I-J) fragments, are the most abundant, whilst siliciclastic rock fragments (mudstone, siltstone and chert; Fig. 4E) only account for minor contributions. Accessory grains types are represented by flakes of micas, both muscovite (Fig. 4I) and biotite. Heavy minerals are scarce and dominated by ultra-stable tourmaline and zircon, whereas rutile and apatite are rare. The framework grains are surrounded by varying proportions of detrital matrix and calcite cement (Fig. 4I-L), with matrix proportions becoming more abundant in the Upper Quartzites unit (Fig. 4K-L). In rare cases the detrital matrix is partially dolomitized. (Fig. 4J). In addition, in quartzose sandstones, authigenic quartz is present in the form of quartz overgrowth that frequently displays sutured contacts of lobate shape (Fig. 4A); it generally makes up less than 5% of quartz.

Modal percentages of essential grain types show significant variations within each investigated stratigraphic interval and between them (Figs. 5 and 6). Quartz generally represents the most abundant grain component, making up an average of 86% of the modal framework in the Lower Quartzites unit, but decreasing up-section towards a mean contribution of 63% in the Upper Quartzites unit. Feldspars account for relatively constant low portions throughout the Lower Quartzites unit (average 4%), but they are more abundant in the Upper Quartzites unit (average 14%). The average lithic fragment count is 10% in the Lower and 22% in the Upper Quartzites unit, respectively. Notwithstanding, the analysis of individual rock fragments contributions (Fig. 6) documents an up-section trend in the Lower Quartzites unit, defined by increasing proportions of sedimentary and volcanic lithic fragments, compensating the up-section decrease of plutonic and low-grade metamorphic fragments. The Upper Quartzites unit records elevated proportions of feldspar grains and plutonic and metamorphic fragments. Noteworthy, an increase in the abundance of mica flakes can be also observed (Fig. 4I). This trend is coupled with the reduction in textural maturity (see Fig. 4 I-L; cf. Diekmann and Wopfner 1995). The increase in mica flakes and the reduced textural maturity are likely to reflect the different proximality of the two sampling locations and not a system-wide change. Hydrodynamic sorting and density differentiation processes along current are documented by various studies (e.g. Lash 1987; Garzanti et al. 2010 and references therein), and this is a typical characteristic of the distal domains of turbidite systems (e.g. Ragusa and Kindler 2018).

The high degree of compositional maturity that characterizes the quartz-rich arenites of the lower part of the Lower Quartzites unit suggests intense sedimentary recycling (e.g. Dickinson et al. 1983; Cox and Lowe 1995; Critelli et al. 2003; Garzanti et al. 2013). This might have occurred due to temporary sediment storage along the source-to-sink pathway, likely in shallow marine environments along the passive margin shelf, where reworking and weathering processes could take effect. This interpretation is similar to the one for the oldest siliciclastic sediments in the San Remo-M. Saccarello Unit proposed by Mueller et al. (2018). The up-section increase in lithic fragments in the Lower Quartzites unit is interpreted to mirror the progressive tectonic uplift and denudation of the sedimentary cover of the provenance terrane. Although there is not a clear breakdown into different petrofacies, the modal composition of sandstones of the Lower and Upper Quartzites units show substantial differences.

While the gradual change from quartzarenites to litharenites defines the evolution of the modal framework of the Lower Quartzites unit, the Upper Quartzites unit is characterized by a further shift towards lithic sub-arkoses (Fig. 5). The increasing abundance of sedimentary and volcanic lithic fragments that characterizes the stratigraphic evolution of the Lower Quartzites unit suggests the growing importance of an eroded terrane comprising a syn-post-rift sedimentary cover sequence, dominantly build up by dolostones and limestone sequences, with minor distributions of volcanic rocks. The differing modal characteristics of the Upper Quartzites unit suggest a slightly different scenario. Here the increased feldspar content points towards a shift in detrital supply with increasing contributions from a basement source.

4.3 Detrital zircon chronology

U-Pb isotopic age determination of 99 ablated spots on 81 detrital zircons (81 core and 18 rims analysed) from the basal sample of the Upper Quartzites unit of the MBS yielded 87 concordant ages (within ±10% of discordance). Full isotopic U-Pb analytical data is presented in the supplementary data file). Representative cathodoluminescence images are illustrated in Fig. 7. Detrital zircon U-Pb ages range from 2683 to 306 Ma (Fig. 8A). The bulk of the ages (>85%) fall into the time interval between 306 and 718 Ma. Two main age populations are observable (Fig. 8B): (1) a dominant component between ca. 306 and 400 Ma (accounting for 39% of detrital ages) and (2) a broad population between ca. 535 and 660 Ma (30%). The dominant age component (1) is defined by the predominance of Upper Devonian to Lower Carboniferous ages (one third of all concordant detrital ages), and is characterized by a high proportion of Tournaisian to Visean zircon ages that range from ca. 335-360 Ma. Within the Cambrian to Cryogenian main age cluster (2), Ediacaran ages are well represented and make up 26% of all ages. Additional ages are represented by an age population between ca. 450 and 490 Ma (Cambro-Ordovician), a minor Tonian age component around 900 Ma, a single "Greenville" concordant age of 1055 Ma and a small population of Paleoproterozoic ages (ca. 1720- 2000 Ma). Due to their wide distribution and low representation (<15%), detrital ages older than 800 Ma disclose minor provenance information.

The broad age population ranging from ca. 535 to 660 Ma is interpreted to correspond to the metamorphic and magmatic stages of the Cadomian orogeny (see e.g. Linnemann et al. 2014; von Raumer et al. 2013). The abundant representation of the Ediacaran age component provides first-order insights into the basement configuration of the source terrane. In the context of the assembly of Gondwana, Ediacaran to Cryogenian ages from metasediments of the Iberian massifs and the Corso-Sardinian Block have been interpreted to reflect a Northern Gondwana heritage (e.g. Avigad et al.

2012; Gutiérrez-Alonso et al. 2015 and references therein). With regards to the pre-Mesozoic basement blocks in the Alpine framework, U-Pb detrital zircon age peaks comparable to the main late Ediacaran peak around 550 Ma have been reported from metaquartzites from Corsica (530-555 Ma age peaks in Cadomian micaschists; Avigad et al. 2018) and, albeit in very low proportions, from Sardinia (Cambrian quartzite of NW Sardinia; Avigad et al. 2012). These ages are interpreted as being derived from Cadomian arcs and coincide with the amalgamation of micro-terranes along the Northern Gondwanan margin (e.g. Stampfli et al. 2011; von Raumer et al. 2015; Franke et al. 2017).

The late Cambrian to Ordovician age population at around 490-440 Ma is interpreted to mirror the gravitational collapse of the Cadomian orogeny and the initiation of the opening of the Palaeo-Tethys rifting stage of the "Rheic Cycle" (e.g. Stampfli et al. 2002b; von Raumer et al. 2003; Sirevaag et al. 2016). Extensional tectonics provided the framework for magmatic episodes that extensively occurred along the Northern Gondwana margin ("Caledonian stage" of Frisch et al. 1984). Magmatism is nonetheless reported from the Penninic basement of both the European Plate (e.g. Franz et al. 2007; Maino et al. 2019) and the Austro-Alpine realm (Frisch et al. 1984).

The main age population from the Upper Devonian to the Upper Carboniferous provides the most significant clue towards a palaeo-European heritage of the source rocks. These ages are interpreted to originate from magmatic and metamorphic events that occurred in the framework of the Variscan cycle (e.g. von Raumer et al. 2003; Ballèvre et al. 2018). Granite emplacements are predominantly documented along the palaeo-European plate (Ballèvre et al. 2018; cf. Giacomini et al. 2007; Dallagiovanna et al. 2009; Casini et al. 2012; Li et al. 2012; Fornelli et al. 2016; Manzotti et al. 2016; Pavanetto et al. 2012; Rubatto et al. 2001, 2011; Sandrone et al. 1993; Williams et al. 2012), whilst minor geochronological constraints on evidence of magmatism from the basement of the Adriatic/Apulian margin exist (Schaltegger and Gebauer 1999; see compilations in Bütler et al. 2010, Beltrán-Triviño et al. 2013 and Manzotti et al. 2015). The comparison of the detrital age fingerprint of the MBS study with that of the older siliciclastic successions of the Western Ligurian Helminthoid Flysch tectonic complex (WLF; Bordighera Sandstones and San Bartolomeo Formation; Fig. 8C) highlights the pronounced similarity in their Variscan age populations, an observation that additionally supports the interpretation of a common source of palaeo-European attribution for the siliciclastic members of the WLF (Mueller et al. 2018).

5 Discussion

5.1 Source terrane considerations

Sandstone compositional data indicate the dominant derivation from the polycyclic sedimentary cover of a continental block. Analysis of the lithic clasts reveals a close similarity to the passive margin sequence of the distal palaeo-European margin (*sensu lato*) of the Alpine Tethys, which comprises the Dauphinois/Provençal domains and the (present-day) adjacent Ligurian Briançonnais terrane (Barale et al. 2017; d´Atri et al. 2017). Although it is straightforward to compare the characteristics of the recycled sedimentary fragments with the stratigraphic make-up of these autochthonous cover sequences, we rule out the proposed Briançonnais provenance (Galbiati 1982; Vanossi et al. 1986; Marini and Terranova 1985). As demonstrated by the widespread Late Cretaceous to Early Tertiary marly pelagic limestones (e.g. "calcschistes planctoniques", "couches rouges"; cf. Michard and Martinotti 2002) which represent the characteristic feature of the Briançonnais post-rift stratigraphic sequence, the Briançonnais terrane was submerged during that time span (Froitzheim et al. 2008; d´Atri et al. 2017), and therefore no erosion of the Briançonnais basement appears to have taken place during time of deposition of the MBS.

The detrital zircon age data from this study are in good correspondence with the crystallization stages recorded in the basement rocks of the Maures-Tanneron Massif (hereinafter MTM), which are represented by polycyclic magmatic and metamorphic suites related to the Cadomian and Variscan orogenies (see Oliot et al. 2015 for a detailed discussion on available age data). The oldest U-Pb zircon age components from the MTM are represented by inherited zircons of orthogneisses dated at 1580 Ma and 1510 Ma (cf. Moussavou 1998). Gneisses from the Internal Zone yielded inherited ages of 630 Ma and 612 Ma, respectively (Moussavou 1998), whilst Innocent et al. (2003) report a Cambrian age of 548 Ma from felsic rocks of the inner part of the Maures basement. The direct provenance assignment to the MTM is primarily based on the match of crystallization ages with zircons within the Late Tournaisian and Visean detrital age component. The oldest granitoid emplacement is dated to the Early Devonian (ca. 404 Ma; Oliot et al. 2015). U-Pb monazite ages of 382 Ma as well as 331 Ma and 329 Ma have been interpreted to mirror stages of crustal thickening in the Early Devonian and in the Visean (Oliot et al. 2015). The latter metamorphic ages concur with granite (338 Ma) and tonalite (334 Ma) emplacement ages in the central and in the eastern Maures Massif (Moussavou 1998). Late Variscan granite intrusions in the Tanneron Massif are documented from both the Tanneron Massif, at 302 Ma and 297 Ma (Demoux et al. 2008) and the Maures batholith, where similar emplacements are dated from the Moulin Blanc Granite (301 Ma) and the Pinet Granite (310 Ma), respectively (Duchesne et al. 2013). Within the latter, inherited zircon ages correspond to crystallization at ca. 512 and 1015 Ma.

The thick, continuous Mesozoic sedimentary succession of the Dauphinois/Provençal domain (Barale et al. 2016 and references therein) reveals further clues towards a detailed provenance classification.

Only a brief summary of the cover sequence is provided here; for a detailed assessment of the stratigraphy and characteristics of the Mesozoic cover sequence of the Ligurian Briançonnais the reader is referred to the comprehensive reviews of Durand (2008) and Barale (2014). The autochthonous cover sequence of the southeastern Provençal domain begins with an Upper Carboniferous continental sedimentary succession that unconformably superimposes the Variscan basement. It comprises reworked granites and metamorphic rocks as well as volcaniclastics deposited in basins adjacent to the MTM (Durand 2008). The Permian stratigraphic succession consists mainly of sandstones and conglomerates in the alluvial Maures graben basin and of subordinate rhyolithic lava flow deposits and effusive tuffs. From the beginning of the Upper Permian to Lower Triassic times, the Provençal domain experienced Buntsandstein-type sedimentation characterized by the presence of a single fluvial system. The Muschelkalk transgression represents the first marine deposits (thin Ladinian dolostones which are superimposed by thick, massive limestones) in the Middle Triassic. The Upper Triassic is represented by pelites and Keuper evaporite deposits which indicate arid conditions (Durand 2008). Following a hiatus from latest Triassic–Lower Jurassic (Barale 2014), thick platform carbonates mark the recommencement of marine sedimentation in the southern Provençal domain from Middle Jurassic to the Lower Cretaceous (Berriasian) times (Barale et al. 2016). The development of a Hauterivian hardground surface, locally overlain by thin pelagic marly limestones, testifies to the drowning of the carbonate platform (Barale et al. 2017).

5.2 Stratigraphic trend in modal composition and significance for passive margin detrital signatures

The petrographic signature of the MBS differs from those of the siliciclastic turbidite systems of the oldest unit of the Western Ligurian Flysch (San Remo Unit), the Bordighera Sandstone (BGS) and its basal complex (Mueller et al. 2018). Notwithstanding, the clastic systems in both units record similar stratigraphic trends, defined by a marked up-section decrease in compositional maturity (Fig. 9). Stampfli et al. (1998) and Michard and Martinotti (2002) propose that coarse-grained sedimentation along the passive European margin was driven by flexural forebulge development and consequent uplift of the lower plate continental margin since the Upper Cretaceous. Mueller et al. (2018) integrate this scenario for the explanation of the supply of coarse sediment of the BGS, allowing for the direct comparison of the compositional evolution of clastic successions sourced from different types of terranes, but deposited in the same geodynamic context.

The composition of the protolith of the sediments dictate the compositional evolution pathway in the provenance discrimination diagrams (Dickinson et al. 1983; cf. Cox and Lowe 1995). Due to their similar geodynamic framework, but divergent stratigraphic organization of the basement rocks and the extent of their sedimentary cover, the successions of the Western Ligurian Flysch complex offer a natural laboratory for the evaluation of models of compositional evolution in comparable uplift scenarios. Both coarse-grained clastic deep-water successions of the Western Ligurian Flysch complex (MBS and BGS) provide an example of the range of detrital signatures that the re-activated passive margin can generate as it approaches the subduction zone (Fig. 9A). The major difference between the MBS and the BGS is that the first-cycle origin of the BGS can be ruled out for the MBS. The abundance of sedimentary and volcanic rock fragments and small proportions of feldspar grains imply the scarcity of exposed crystalline rocks in the source area. The BGS display the compositional and textural characteristics of first-cycle sandstones and represent a sequence derived from a stable cratonic (shelf?) setting (as represented by the basal complex sands) first and subsequently from a progressively uplifted basement block (Fig. 9B). In this scenario tectonic instability of the craton is illustrated by the modal evolution along the QtF limb. By contrast, the recycling-dominated sedimentation recorded by the MBS is representative for a setting in which the progressively reduced mineralogical maturity of the uplifted stable cratonic margin sequence is illustrated by the evolution along the QtL limb of the provenance ternary diagram (Fig. 9C), illustrating the re-activation of a passive margin segment that experienced high subsidence and sedimentation rates mostly during pre-syn rifting stages.

5.3 Towards a provenance signature of the Southern European Tethyan Palaeomargin?

The new detrital zircon ages obtained in this study, in combination with the lithic fragment types (which provide the direct link towards the Mesozoic cover sequence), reveal the palaeo-European origin of the clastic detritus. This suggests that the Borghetto d´Arroscia-Alassio Unit was sourced from recycled sediments of the catchment area of the Variscan Maures-Tanneron Massif which represents the northern continuation of the Corso-Sardinian Block microcontinent (Rossi et al. 2009). The proposed Ligurian Briançonnais source (Vanossi, 1962; Galbiati, 1986; Marini and Terranova, 1985) could not be confirmed. The detrital zircon age spectra match the crystallization events recorded in the Provencal domain of the southern Variscan belt and thus have the potential to serve as a tracer for detrital provenance from the southern part of the southern palaeo-European Tethyan margin domain.

The detrital zircon age distributions of Permo-Carboniferous metasediments of the Pinerolo Unit and the Permian Zone Houillère (Manzotti 2016) show significant commonalities with that of the MBS (Fig. 10). With respect to the dominant age populations between 300-350 Ma and the broad peak between ca. 500-650 Ma, the samples from the Pinerolo Unit are almost identical to the one analysed in this study. The Pinerolo Unit is exposed in a window beneath the Dora Maira Nappe and comprises a basement made up of late-Variscan granitoid bodies and a Permo-Carboniferous sedimentary cover

(Avigad et al. 2003; Froitzheim et al. 2008). Notably, the detrital ages of the Pinerolo Unit are characterized by the absence of ages younger than 300 Ma, whereas this age population is well-expressed in the detrital spectra of the Zone Houillère sediments. Manzotti et al. (2016) favour a common provenance for both the Pinerolo Unit and the Permian Zone Houillère, represented by the palaeo-European Variscan basement units (i.e. the External Massifs, the Maures-Tanneron Massif, the Corsican-Sardinian Massif). Although the older Cambro-Ordovician age peaks are equally present in the detrital zircon age spectra of late Carboniferous-early Permian metasedimentary rocks proposed to be sourced from the Briançonnais domain (Money Zone of the Gran Paradiso Unit; Manzotti et al. 2015), the detrital record of the Briançonnais appears to be characterized by the absence of Upper Carboniferous ages. Manzotti et al. (2015) interpret this sparse representation of Upper Carboniferous crystallisation ages as a distinguishing feature of the Briançonnais domain (see also Ballèvre et al. 2018), and suggest that the similarities of the Briançonnais with the Adriatic palaeomargin exceed those with its European counterpart.

In accordance with the new petrographic and chronologic results presented in this study, we regard the age signature recorded in both the Pinerolo Unit and in the Monte Bignone sediments as representing the detrital zircon age fingerprint of the Southern European Tethyan palaeomargin. Taking into account the still poorly constrained displacement of palaeo-European terranes, Penninic basement blocks and metasedimentary sequences by out-of-sequence thrusting (e.g. Froitzheim et al. 2008; Handy et al. 2010), and the debated palaeogeographic position of the Briançonnais continental fragment (e.g. Dal Piaz et al. 2003; Froitzheim et al. 2008; Handy et al. 2010; Manzotti et al. 2015), the identification of distinct source terrane detrital signatures can aid to further untangle the Western Alps tectonic puzzle. A comparison of the new detrital zircon age data with those from several published datasets has been performed by means of the multidimensional scaling (MDS) method (Vermeesch et al. 2013). This approach converts the dissimilarities between samples into distance in non-dimensional space (Vermeesch 2013) and creates a dimensionless arrangement of the sample points in which in a Cartesian coordinate system similar samples cluster together (Saylor et al. 2017). MDS visualization has proven to represent a valuable tool in provenance analysis, since it provides constraints on the role of pre-orogenic tectonic units in providing sediment (Stephan et al. 2018). Twenty-nine detrital age datasets (2955 individual detrital zircon ages) of representative siliciclastic successions deposited in the framework of the Alpine tectono-sedimentary cycle (e.g. Beltrán-Triviño et al. 2013; Cassinis et al. 2018) have been considered (Fig. 11). The compiled dataset comprises available detrital zircon age data of clastic sequences deposited in both the Piedmont-Ligurian oceanic domain and in the European foreland basin. Published source works comprise: detrital zircon ages from successions derived from the Inner (Manzotti et al. 2015) and External Crystalline Massifs

(Manzotti et al. 2016) as well as from the Briançonnais terrane (Chu et al. 2016); detrital zircon ages for the Western Ligurian Flysch (Mueller et al., 2018); a detrital zircon dataset from the Corsica Nappes (Lin et al. 2018); detrital zircon data from the Elba Verruco Flysch (Sirevaag et al. 2016); detrital zircon ages for the European Foreland Basin (Grès de Champsaur and Flysch des Aiguilles d'Arves) and the cover of ophiolite nappes deposited in the Piedmont-Ligurian Ocean (Schistes Lustrès) from Chu et al. (2016); and finally detrital zircon data of Southern Alps and Austro-Alpine successions (Beltrán-Triviño et al. 2013).

The MDS plot illustrates a distinct cluster of sedimentary successions sourced from the pre-Alpine Internal and External Massifs and various micro-terranes of palaeo-European affinity (green outline; Fig. 11). However, some close vicinity is observable between successions derived from the Austro-Alpine domain with successions interpreted to be representative of Southern Alps provenance (Austroalpine Altein, Buchenstein and Prosanto Formations with the Southern Alps-derived Val Sabbia Fm.; Austroalpine Fuorn and Southern Alps Dasdana Fms.; as well as the Salluver and Bellano Fms., respectively; all data from Beltrán-Triviño et al. 2013). Remarkably, some flysch formations incorporated into the Corsican Balgane and Piedmont Nappes (Narbinco Flysch and Tralonca Flysch Fms., respectively) of previously unassigned provenance (cf. Lin et al. 2018), show closer similarity towards the Apulian/Adriatic plate. In view of the growing body of detrital zircon studies, this approach can potentially become an indispensable tool for solving tectonic and palaeogeographic problems in the debated pre-collisional framework of the Alps-Apennine orogenic system.

6 Conclusions

The results of the multi-proxy sediment provenance study of the Monte Bignone Sandstones (MBS) of the Western Ligurian Flysch complex contribute to a better understanding of the pre-collisional evolution of the Piedmont-Ligurian Ocean and the controversial geodynamic history of its bounding margins. The main findings can be summarized as the following:

- Measurement of palaeocurrent indicators reveals a primarily eastward transport of proximal slope channel-fill sediments. Restoration of the ca. 45-50° counter-clockwise rotation related to the opening of the Liguro-Provençal Basin illustrates a sediment source situated at the northern Tethyan margin.

- MBS sandstone modal composition suggests an up-section increase in the importance of an eroded sedimentary cover of a continental terrane as the source for the clastic sediments. This portrays the progressive erosion of a passive margin segment characterized by a thick pre-syn rift Mesozoic sedimentary cover.

- Based on the results of detrital zircon chronology, the source area of the MBS can be narrowed to have been located along the European Tethyan Palaeomargin. Considering the strong representation of Tournaisian and Visean detrital ages within the Variscan detrital age component, reworked sediments staged from the Maures-Tanneron Massif most likely provided the major contribution of detrital zircons into the catchment area of the MBS.

- In the context of Alpine subduction, these results strengthen the hypothesis that the siliciclastic pre-collisional turbidite systems along the Western part of the subduction system were derived from the re-activated margin of the down-bending European continental block while it was approaching the subduction zone.

- The comparison of the new geochronological age signatures of this study with detrital age distributions from published datasets of the Western Alps by means of non-metric multidimensional scaling (MDS) analysis yields a distinct cluster of the palaeo-Europe-derived successions. Considering the tectonically complex make-up of the Alpine Nappe pile, this palaeo-European detrital zircon age signature has the potential of providing an accurate tool for linking sedimentary successions to their sediment sources and therefore allowing refined reconstructions of the geologic histories of the bounding Tethyan margins.

Acknowledgements

Financial support for this research was provided by the University of Pavia research grant to P. Mueller. Field work was supported by funding provided by the Turbidite Research Group sponsors: AkerBP, BP, ConocoPhilips, Equinor, Eni, Hess, Murphy Oil Corporation, OMV and Shell. We are grateful to M. Zattin (University of Padova) for the heavy mineral separation and to M. Palenzona (CNR Pavia) for assistance with CL images. We thank U. Linnemann and an anonymous reviewer for their helpful suggestions that improved the manuscript. Journal editors W.-C. Dullo and T. Voigt are thanked for their corrections and editorial handling.

7 References

Avigad D, Chopin C, Le Bayon R (2003) Thrusting and extension in the Southern Dora-Maira Ultra-High-Pressure Massif (Western Alps): view from below the coesite-bearing unit. J. Geol. 111:57–70

Avigad D, Gerdes A, Morag N, Bechstädt T (2012) Coupled U–Pb–Hf of detrital zircons of Cambrian sandstones from Morocco and Sardinia: implication for provenance and Precambrian crustal evolution of North Africa. Gondwana Res. 21:690–703

Avigad D, Rossi, P, Gerdes A, Abbo A (2018) Cadomian metasediments and Ordovician sandstone from Corsica: detrital zircon U–Pb–Hf constrains on their provenance and paleogeography. Int. J. Earth Sci 107:2803–2818

Ballèvre M, Manzotti P, Dal Piaz GV (2018) Pre-Alpine (Variscan) inheritance: A key for the location of the future Valaisan Basin (Western Alps). Tectonics 37:786–817

Barale, L (2014) The Meso-Cenozoic stratigraphic succession adjoining the Argentera Massif: stratigraphic, sedimentologic and diagenetic evidence of syndepositional tectonics. Stratigraphy. Dissertation, Universita degli Studi di Torino, 240 pp.

Barale L, d'Atri A, Piana F (2016) The Meso–Cenozoic stratigraphic succession of the Col de Braus area (Maritime Alps, SE France), Journal of Maps 12(5):804-814

Barale L, Bertok C, d'Atri A, Martire L ,Piana F (2017) -Stratigraphy, sedimentology and syndepositional tectonics of the Jurassic-Cretaceous succession at the transition between Provençal and Dauphinois domains (Maritime Alps, NW Italy). Riv. It. Paleontol. Strat. 123: 355-378.

Beltrán-Triviño A, Winkler W, von Quadt A (2013) Tracing Alpine sediment sources through laser ablation U–Pb dating and Hf-isotopes of detrital zircons. Sedimentology 60:197–224

Bertok C, Martire L, Perotti E, d'Atri A, Piana F (2012) Kilometre-scale palaeoescarpments as evidence for Cretaceous synsedimentary tectonics in the External Briançonnais Domain (Ligurian Alps, Italy). Sed. Geol. 251-252:58-75

Boni A, Vanossi M (1960) Ricerche e considerazioni sul flysch della Liguria occidentale. Atti Ist. Geol. Univ. Pavia 11:31-178

Boni A, Vanossi M (1972) Carta geologica dei terreni compresi tra il Brianzonese Ligure s.l. ed il Flysch ad Elmintoidi s.s. Atti Ist. Geol. Univ. Pavia 23 , carta allegata, Pavia.

Bracciali L, Marroni M, Pandolfi L, Rocchi S, (2007) Geochemistry and petrography of Western Tethys Cretaceous sedimentary covers (Corsica and Northern Apennines): from source area to configuration of margins. In: Arribas J, Critelli S, Johnsson MJ (eds.), Sedimentary Provenance and Petrogenesis: Perspectives From Petrography and Geochemistry. GSA Special Paper 420:73–93

Caron C, Homewood P, Wildi W (1989) The Original Swiss Flysch: A reappraisal of the Type Deposits in the Swiss Prealps. Int. J. Earth Sci 26:1–45

Carrapa B (2010) Resolving tectonic problems by dating detrital minerals. Geology 38:191-192

Carrapa, B., Di Giulio, A., Mancin, N., Stockli, D., Fantoni, R., Hughes, A., Gupta, S., 2016. Tectonic significance of Cenozoic exhumation and foreland basin evolution in the Western Alps, Tectonics 35:1892–1912

Casini L, Cuccuru S, Maino M, Oggiano G, Tiepolo M (2012) Emplacement of the Arzachena Pluton (Corsica–Sardinia Batholith) and the geodynamics of incoming Pangaea. Tectonophysics 544-545:31–49

Cassinis G, Perotti C, Santi G (2018). Post-Variscan Verrucano-like deposits in Italy, and the onset of the alpine tectono-sedimentary cycle. Earth-Sci. Rev. 185:476-497

Chu Y, Lin W, Faure M, Wang Q (2016) Detrital zircon U-Pb ages and Hf isotopic constraints on the terrigenous sediments of the Western Alps and their paleogeographic implications. Tectonics 35:1-20

Cox R, Lowe DR (1995) A Conceptual Review of Regional Scale Controls on the Compositions of Clastic Sediments and the Co-Evolution of Continental Blocks and Their Sedimentary Cover. J. Sed. Res. 65:1-12

Critelli S, Arribas J, Le Pera E, Tortosa A, Marmaglia KM, Latter, KK (2003) The recycled orogenic sand provenance from an uplifted thrust belt, Betic Cordillera, southern Spain: J. Sed. Res. 73:72–81

Dal Piaz GV (1999) The Austroalpine–Piedmontnappe stack and the puzzle of Alpine Tethys. Mem. Sci. Geol. Padova 51:155–176

Dal Piaz GV, Bistacchi A, Massironi M (2003) Geological outline of the Alps. Episodes 26:175–180

D´Atri, A, Piana F, Barale L, Bertok C, Martire L (2016) Geological setting of the southern termination of Western Alps. Int. J. Earth Sci. 105:1831–1858

Decarlis A, Beltrando M, Manatschal, G, Ferrando S, Carosi R (2017) Architecture of the distal Piedmont-Ligurian rifted margin in NW Italy: Hints for a flip of the rift system polarity. Tectonics 36:2388–2406

Di Giulio, A. (1985) Sull'eta terziaria dei Calcari di Ubaga, Successione di Borghetto d'Arroscia-Alassio (Alpi Marittime). Riv. It. Paleont. Strat. 92:251-260

Di Giulio A (1992) The evolution of the Western Ligurian Flysch Units and the role of mud diapirism in ancient accretionary prisms (Maritime Alps, Northwestern Italy). Int. J. Earth Sci. 81:655-668

Di Giulio A, Galbiati B (1991) Le facies caotiche della Liguria occidentale: un nuovo modello interpretativo. Atti Ticinensi Sci. Terra 34:155–160

Di Giulio A, Ronchi A, Sanfilippo A, Balgord EA, Carrapa B, Ramos VA (2017) Cretaceous evolution of the Andean margin between 36°S and 40°S latitude through a multiproxy provenence analysis of Neuquen Basin strata (Argentina). Basin Res. 29/3:284-304

Di Giulio, A., Valloni, R., 1992. Analisi microscopia delle arentiti terrigene: parametri petrologici e composizioni modali. Acta Naturalia de l´Ateneo Parmese 28:55–101

Dickinson WR (1970) Interpreting detrital modes of graywacke and arkose. J. Sed. Petr. 40 (2):695–707

Dickinson WR (1985) Interpreting provenance relations from detrital modes of sandstones. In: Zuffa, G.G. (Ed.), Provenance of arenites: 165–189, NATO ASI Ser., Dordrecht (Reidel).

Dickinson WR, Suczek C (1979) Plate tectonics and sandstone compositions. AAPG Bulletin 63:2164–2182

Dickinson WR, Valloni R (1980) Plate settings and provenance of sands in modern ocean basins. Geology 8:82–86

Dickinson WR, Gehrels, GE (2009) Use of U-Pb ages of detrital zircons to infer maximum depositional ages of strata: A test against a Colorado Plateau Mesozoic database. Earth Planet. Sci. Lett. 288:115-125

Diekmann B, Wopfner H (1996) Petrographic and diagenetic signatures of climatic change in periand postglacial Karoo Sediments of SW Tanzania. Palaeogeogr., Palaeoclimatol., Palaeoecol. 125:5–25

Duchesne JC, Liégois JP, Bolle O, Vander Auwera J, Bruguier O, Matukov DI, Sergeev SA (2013) The fast evolution of a crustal hot zone at the end of a transpressional regime: The Saint-Tropez peninsula granites and related dykes (Maures Massif, SE France). Lithos 162–162:195–220

Dunkl I, Di Giulio A, Kuhlemann J (2001) Combination of single-grain fission track chronology and morphological analyses of detrital zircon crystals in provenance studies – origin of the Macigno Formation (Apennines, Italy). J. Sed. Res. 71:515-524

Durand, M (2008) Permian to Triassic continental successions in southern Provence (France): an overview. Boll. Soc. Geol. It. 127(3):697-716

Fonneland HC, Lien T, Martinsen OJ, Pedersen, R.B., Kosler J (2004) Detrital zircon ages: a key to understanding the deposition of deep marine sandstones in the Norwegian Sea. Sed. Geol. 164:147-159

Fornelli A, Micheletti F, Piccarreta G (2016) Late-Proterozoic to Paleozoic history of the peri-Gondwana Calabria–Peloritani Terrane inferred from a review of zircon chronology. Springerplus 5:1-19

Franke W, Robin M, Cocks L, Torsvik TH (2017) The Palaeozoic Variscan oceans revisited. Gondwana Res. 48:257-284

Franz L, Romer RL (2007) Caledonian high-pressure metamorphism in the Strona-Ceneri Zone (Southern Alps of southern Switzerland and northern Italy). Swiss J. Geosc. 100:457-467

Frisch W, Neubauer F, Satir M (1984) Concepts of the evolution of the Austroalpine basement complex (Eastern Alps) during the Caledonian-Variscan cycle. Int. J. Earth Sci. 73:47–68

Froitzheim N, Plasienka D, Schuster R 2008 Alpine tectonics of the Alps and Western Carpathians. In: McCann, T. (ed.), The Geology of Central Europe. Volume 2: Mesozoic and Cenozoic, Geol. Soc. Publ., London, 1141-1232.

Galbiati B (1982) Nuovi dati e considerazioni sull'elemento di Borghetto d'Arroscia (Alpi liguri). Rend. Soc. Geol. It., 4:339-341

Galbiati B (1986) L'unità di Borghetto d'Arroscia-Alassio. Mem. Società Geol. d'Italia, 28:181-210.

Garzanti E, Andò S, Vezzoli G (2006) The Continental Crust as a Source of Sand (Southern Alps Cross Section, Northern Italy). J. Geol. 114:3–554

Garzanti E, Doglioni C, Vezzoli G, Ando S (2007) Orogenic belts and orogenic sediment provenance. J. Geol. 115:315-334

Garzanti E, Ando S, France-Lanord C, Vezzoli G, Censi P, Galy V, Najman Y (2010) Mineralogical and chemical variability of fluvial sediments 1. Bedload sand (Ganga–Brahmaputra, Bangladesh). Earth Planet. Sci. Lett. 299:368–381

Garzanti E, Limonta M, Resentini A, Bandopadhyay PC, Najman Y, Andò S, Vezzoli G (2013) Sediment recycling at convergent plate margins (Indo-Burman Ranges and Andaman-Nicobar Ridge). Earth-Sci. Rev. 123:113-132

Gazzi P (1966) Le arenarie del flysch sopracretaceo dell'Appenino modenese: correlazioni con il flysch di Monghidoro: Mineral. Petrogr. Acta12:69-97

Gehrels G (2011) Detrital zircon U-Pb geochronology: Current methods and new opportunities. Tectonics of sedimentary basins: Recent advances:45-62

Giacomini F, Braga R, Tiepolo M, Tribuzio R (2007) New constraints on the origin and age of Variscan eclogitic rocks (Ligurian Alps, Italy). Contrib. Mineral. Petrol. 153:29–53

Giorgis D, Thélin P, Stampfli M, Bussy F (1999) The Mont-Mort metapelites: Variscan metamorphism and geodynamic context (Briançonnais basement, Western Alps, Switzerland). Schweiz. Mineral. Petrogr. Mitt. 79:381-398

Gutiérrez-Alonso G, Fernández-Suárez J, Pastor-Galán D, Johnston, ST, Linnemann U, Hofmann M, Shaw J, Colmenero JR, Hernández P (2015) Significance of detrital zircons in Siluro-Devonian rocks from Iberia. J. Geol. Soc. Lond. 172:309–322

Handy MR, Schmid SM, Bousquet R, Kissling E, Bernoulli D (2010) Reconciling plate-tectonic reconstructions of Alpine tethys with the geological record of spreading and subduction in the Alps. Earth-Sci. Rev. 102:121–158

Homewood P, Laveltin O (1988) Classic swiss clastics (flysch and molasse): The Alpine connection. Geodinamica Acta 2:1-11.

Ingersoll RV, Bullard, TF, Ford RD, Grimm JP, Pickle JD, Sares SW (1984) The effect of grain size on detrital modes: a test of the Gazzi-Dickinson point-counting method. J. Sed. Petrol. 54:103–116

Innocent C, Michard A, Guerrot C (2003) U-Pb zircon age of 548 Ma for the leptynites (high grade felsic rocks) of the central part of the Maures massif. Geodynamic significance of the so-called leptyno-amphibolitic complexe of the Varsican belt of western Europe. Bull. Soc. Géol. Fr. 174: 585-594

Jackson SE, Pearson, NJ, Griffin WL, Belousova EA (2004) The application of laser ablation-inductively coupled plasma-mass spectrometry to in situ U–Pb zircon geochronology. Chem. Geol. 211:47–69

Lanteaume M (1962) Contribution à l'étude géologique des Alpes Maritimes franco-italiennes. Thèse Sc. Nat., Paris, n° 4649, 413 p.

Lanteaume M, Radulescu N, Gavos M, Feraud J (1990) Notice explicative, Carte Géol. De France (1/50.000), feuille Viève-Tende (948). Orleans: BRGM. 139 pp.

Lash GG (1987) Longitudinal petrographic variations in a Middle Ordovician trench deposit, central Appalachian Orogen. Sedimentology 34:227–235

Lihou JC, Mange-Rajetzky MA (1996) Provenance of the Sardona Flysch, Eastern Swiss Alps: example of high-resolution heavy mineral analysis applied to an ultrastable assemblage. Sed. Geol. 105:141-157

Lin W, Rossi P, Faure M, Li, X-H, Ji W, Chu Y (2018) Detrital zircon age patterns from turbidites of the Balagne and Piedmont nappes of Alpine Corsica (France): evidence for an European margin source. Tectonophysics 722:69–105

Linnemann U, Pereira F, Jeffries TE, Drost K, Gerdes A (2008). The Cadomian Orogeny and the opening of the Rheic Ocean: The diachrony of geotectonic processes constrained by LA-ICP-MS U–Pb zircon dating (Ossa-Morena and Saxo-Thuringian Zones, Iberian and Bohemian Massifs). Tectonophysics 461:21–43

Lopez Jimenez R, Cronin BT, Turner CC, Celik H, Bastidas R, Kneller BC (2018). The Alikayasi Canyon-Channel System (Miocene, SE Turkey) compared with the South Brae Fan System (Upper Jurassic, North Sea): Characterising sand and gravel filled channel complexes in coarse-grained deep-water systems without gravel cone geometries. In Turner CC, Cronin BT, editors, Rift-related coarse-grained submarine fan reservoirs: the Brae Play, South Viking Graben, North Sea: AAPG Memoir, p. 595-618

Maffione M, Speranza F, Faccenna C, Cascella A, Vignaroli G, Sagnotti L (2008). A synchronous Alpine and Corsica–Sardinia rotation. J. Geophys. Res. 113(B03104)

Maino M, Casini L, Ceriani A, Decarlis A, Di Giulio A, Seno S, Setti M, Stuart FM (2015) Dating shallow thrusts with zircon (U-Th)/He thermochronometry — the shear heating connection. Geology 43:495–498

Maino M, Gaggero L, Langone A, Seno S, Fanning M (2019) Cambro-Silurian magmatism at the northern Gondwana margin (Penninic basement of the Ligurian Alps). Geosci. Front. 10:315-330

Manzotti P, Poujol M, Ballèvre M (2015) Detrital zircon geochronology in blueschist-facies meta-conglomerates from the Western Alps: Implications for the late Carboniferous to early Permian palaeogeography. Int. J. Earth Sci. 104:703–721

Manzotti P, Ballèvre M, Poujol M (2016) Detrital zircon geochronology in the Dora Maira and Zone Houillère: A record of sediment travel paths in the Carboniferous. Terra Nova 28:279–288

Marini M, Terranova R (1985) Nuovi dati sulla litostratigrafia dei flysch della Liguria occidentale e sui loro rapporti strutturali. Atti Soc. Tosc. Sc. Nat. 92:95-163

Marini M, Milli S, Ravnas R, Moscatelli A, (2015) A comparative study of confined vs. semi-confined turbidite lobes from the Lower Messinian Laga Basin (Central Apennines, Italy): Implications for assessment of reservoir architecture. Mar. Petr. Geol. 63:142-165

Marroni M, Meneghini F, Pandolfi L (2010) Anatomy of the Ligure-Piemontese subduction system: evidence from Late Cretaceous–middle Eocene convergent margin deposits in the Northern Apennines, Italy. Int. Geol. Rev. 52:1160-1192

Michard A, Martinotti G (2002) The Eocene unconformity of the Briançonnais domain in the French—Italian Alps, revisited (Marguareis massif, Cuneo): a hint for a Late Cretaceous—Middle Eocene frontal bulge setting. Geodin. Acta 15:5-6

Moussavou M (1998) Contribution à l'histoire thermo-tectonique varisque du massif des Maures par la typologie du zircon et la géochronologie U/Pb sur minéraux accessoires. PhD Thesis, University of Montpellier 2, 187 p.

Mueller P, Langone A, Patacci M, Di Giulio A (2018) Detrital signatures of impending collision: The deep-water record of the Upper Cretaceous Bordighera Sandstone and its basal complex (Ligurian Alps, Italy). Sediment. Geol. 377:147-161

Oliot E, Melleton J, Schneider J, Corsini M, Gardien V, Rolland Y (2015) Variscan crustal thickening in the Maures-Tanneron massif (South Variscan belt, France): new in situ monazite U-Th-Pb chemical dating of high-grade rocks. Bull. Soc. Géol. France 186:145-169

Patacci, M. (2016). A high-precision Jacob's staff with improved spatial accuracy and laser sighting capability. Sediment. Geol. 335: 66-69.

Pavanetto P, Funedda, A, Northrup CJ, Schmitz M, Crowley J, Loi A (2012) Structure and U–Pb zircon geochronology in the Variscan foreland of SW Sardinia, Italy. Geol. J. 47:426–445

Perotti M, Andreucci B, Talarico F, Zattin M, Langone A (2017) Multi-analytical provenance analysis of Eastern Ross Sea LGM till sediments (Antarctica): Petrography, geochronology, and thermochronology detrital data. Geochem. Geophys. 18 (6):2275-2304

Ragusa J, Kindler P, Segvic B, Ospina-Ostios LM (2017). Provenance analysis of the Voirons Flysch (Gurnigel nappe, Haute-Savoie, France): stratigraphic and palaeogeographic implications. Int. J. Earth Sci. 106:2619–2651

Ragusa J, Kindler P (2018). Compositional variations in deep-sea gravity-flow deposits. A case study from the Voirons Flysch (Voirons-Wägital complex, Chablais Prealps, France). Sediment. Geol. 377:111-130

Rossi P, Oggiano G, Cocherie A (2009) A restored section of the “southern Variscan realm” across the Corsica–Sardinia microcontinent. C. R. Gèoscience 341: 224-238

Saylor JE, Jordan JC, Sundell KE, Wang X, Wang S, Deng T (2017) Topographic growth of the Jishi Shan and its impact on basin and hydrology evolution, NE Tibetan Plateau. Basin Res. 30:544-563

Schaltegger U, Gebauer D (1999) Pre-Alpine geochronology of the Central, Western and Southern Alps. Schweiz. Mineral. Petrogr. Mitt. 79: 79-87

Seno S, Dallagiovanna G, Vanossi, M (2005) Pre-Piedmont and Piedmont-Ligurian nappes in the central sector of the Ligurian Alps: a possible pathway for their superposition on to the inner Briançonnais units. Bollett. Soc. Geol. Italiana 124 (2): 455-464

Shaw J, Gutiérrez-Alonso G, Johnston S, Pastor-Galán D (2014) Provenance variability along the early Ordovician north Gondwana margin: Paleogeographic and tectonic implications of U-Pb detrital zircon ages from the Armorican Quartzite of the Iberian Variscan belt. GSA Bulletin 126:702-719

Sirevaag H, Jacobs J, Ksienzyk AK, Rocchi S, Paoli G, Jørgensen GH, Košler, J (2016) From Gondwana to Europe: the journey of Elba Island (Italy) as recorded by U/Pb detrital zircon ages of Paleozoic metasedimentary rocks. Gondwana Res. 38:273–288

Sláma J, Kosler J, Condon DJ, Crowley JL, Gerdes A, Hanchar JM, Horstwood MSA, Morris GA, Nasdala L, Norberg N, Schaltegger U, Schoene B, Tubrett MN, Whitehouse MJ (2008): Plesovice zircon - a new natural reference material for U-Pb and Hf isotopic microanalysis. – Chem. Geol. 249(1-2):1—35

Stampfli GM, Borel GD, Marchant R, Mosar J (2002a) Western Alps geological constraints on western Tethyan reconstructions. J. Virt. Explorer 8:77–106

Stampfli GM, von Raumer J, Borel G (2002b) The Paleozoic evolution of pre-Variscan terranes: from Gondwana to the Variscan collision. GSA Spec. Publ. 364:263–280

Stampfli GMM, Mosar J, Marquer D, Marchant R, Baudin T, Borel G (1998) Subduction and obduction processes in the Swiss Alps. Tectonophysics 296:159-204

Stampfli GM, von Raumer J, Wilhem C (2011) The distribution of Gondwana derived terranes in the early Paleozoic. In: Gutiérrez-Marco JC, Rábano I, García-Bellido D (eds.) The Ordovician of the world, Cuadernos del Museo Geominero, Instituto Geológico y Minero de España, Madrid 14:567–574

Stanley DJ (1965) Heavy minerals and provenance of sands in flyschof central and southern French Alps. AAPG Bulletin 49:22-40

Stephan T, Kroner U, Romer RL (2019) The pre-orogenic detrital zircon record of the Peri-Gondwanan crust. Geol. Mag. 156(2):281-307

Thomas WA, (2011) Detrital-zircon geochronology and sedimentary provenance. Lithosphere 3:304-308

Thum L, De Paoli R, Stampfli GM, Moix, P (2015) The Piolit, Pelat and Baiardo Upper Cretaceous flysch formations (western Alps): Geodynamic implications at the time of the Pyrenean tectonic phases. Bull. Soc. Géol. France, 2015 186:209-221

Valloni R, Zuffa GG (1984) Provenance changes for arenaceous formations of the northern Apennines, Italy. GSA Bulletin 95:1035–1039

Van Achterbergh E, Ryan CG, Jackson SE, Griffin WL (2001) Data reduction software for LA- ICP- MS. Laser- Ablation- ICPMS in the earth sciences — Principles and applications, Mineralog. Assoc. Canada Short Course Series 29:239–243

Vanossi M, Cortesogno L, Galbiati B, Messiga B, Piccardo G, Vannucci R (1986) Geologia delle Alpi Liguri: dati, problemi, ipotesi. Mem. Soc. Geol. It. 28:5-75

Vermeesch P (2012) On the visualisation of detrital age distributions. Chem. Geol. 312:190-194

Vermeesch P (2018) IsoplotR: A free and open toolbox for geochronology. Geosci. Front. 9:1479-1493

Vezzoli G, Garzanti E, Monguzzi S (2004) Erosion in the Western Alps (Dora Baltea basin). 1. Quantifying sediment provenance. Sed. Geol. 171:227-246

Von Raumer JF, Stampfli GM, Borel G, Bussy F (2002) Organization of pre-Variscan basement area at the north-Gondwanan margin. Int. J. Earth Sci. 91:35–52

Von Raumer JF, Stampfli GM, Bussy F (2003) Gondwana-derived microcontinents-the constituents of the Variscan and Alpine collisional orogens. Tectonophysics 365:7–22

Von Raumer JF, Stampfli GM, Arenas R, Sánchez Martínez S (2015) Ediacaran to Cambrian oceanic rocks of the Gondwana margin and their tectonic interpretation. Int. J. Earth Sci. 104:1107–1121

Wiedenbeck M, Alle P, Corfu F, Griffin WL, Meier M, Oberli F, Von Quadt A, Roddick, JC, Spiegel W (1995) Three natural zircon standards for U–Th–Pb, Lu–Hf, trace element and REE analyses. Geostandard Newslett. 19:1–23

Wildi W (1985) Heavy mineral distribution and dispersal pattern in penninic and ligurian flysch basins (Alps, northern Apennines). Giorn. Geol. 47:77-99

Figure captions

Fig. 1. (A) Location of the study area in the framework of the Western Alps. (B) Geological map of the Western Ligurian Flysch Complex and its surrounding tectonic units. ATF: Alpine Thrust Front; E-U: Embrunais-Ubaye nappe; WLF: Western Ligurian Flysch nappe; TH-M: Torino Hills and Monferrato High; TPB: Tertiary Piedmont Basin. (C) Schematic geological map of the Moglio-Testico, Borghetto d´Arroscia and Colla Domenica-Leverone Units of the Western Ligurian Flysch complex. Red stars indicate sampled sections at localities “Capo Croce” (Samples PA 01-27) and (B) “Ubaghetta” (see Fig. 2 for details). Modified from Boni and Vanossi (1972), Lanteaume et al (1990), Di Giulio (1992) and Maino et al (2015).

Fig. 2. Summary logs of the Borghetto Unit in the proximal (A) and distal (B) domain (modified from Galbiati 1986). Insets show detailed logs at Capo Croce (C) and Ubaghetta (D) and the stratigraphic position of sandstone samples PA_1 to PA_27 (diamonds) and UR_01 to UR_03 (triangles). Position of detrital zircon samples QdMZ_1 and QdMZ_2 are also highlighted. Rose diagrams represent palaeocurrent indicators from detailed logs (black: groove casts; white: flute casts, ripples and cross-bedding foresets).

Fig. 3. Outcrop examples of the Monte Bignone Sandstones. A) Medium- to thick-bedded strata from the Lower Quartzites unit in the proximal sample location “Capo Santa Croce”. View towards SSE. Note the eastward dipping of foresets of cross-bedded strata. B) Sampled outcrop of the Upper Quartzites unit close to “Ubaghetta”. Location of the sample processed for detrital zircon chronology is indicated with an orange star. C) Chaotic body within the pelitic member in the distal outcrop “Ubaghetta”. D) Representative strata of the “middle” conglomerates, characterized by poorly sorted polymict gravel conglomerate dominated by calcareous clasts. Locality “Capo Santa Croce”.

Fig. 4. Representative photomicrographs of the thin sections investigated under crossed nichols. Samples from the Lower Quartzites unit (A-H). A) Almost pure quartzitic composition characterizing the basal part of the Lower Quartzites unit in the “Capo Santa Croce” sample location. Note the quartz overgrowth (arrows). B) Quartz aggregate (dashed patch) in orthoquartzite sample. C) Feldspar varieties (microcline and albite) observed in sample PA_12. Note the partial dissolution of the lamellae in the perthitic alkali feldspar grain (Fp). D) Assemblage of lithic fragments types: fine-grained sandstone lithic fragment (Ls) together with low-grade metamorphic lithic fragment (Lm). E)

Association of lithic clasts (volcanic (Lv), sedimentary (siltstone; Ls) and lithic-plutonic (Lp) fragments) and mono- and polycrystalline quartz varieties in sample PA_13. F) Rhyolithic volcanic fragment (Lv) characterized by K-feldspar phenocrysts (arrows) floating in porphyric matrix in assemblage with quartz grains and sedimentary lithic fragments G) Sample PA_19 characterised by abundant dolostone fragments (ds). H) Poor degree of sorting that characterises the topmost samples of the Lower Quartzites unit. Note the angularity of grains and the high abundance of detrital matrix. CE: carbonatic lithic fragment; CEm: micritic limestone lithic fragment. Samples from the Upper Quartzites unit (I-L). I) Mica flakes (yellow arrows) in texturally and compositionally immature lithic arenites characteristic of the lowermost part of the Upper Quartzites unit. J) Poorly sorted litharenite. Note the partial dolomitization of the matrix (yellow arrows). K) Examples of texturally immature samples from the Upper Quartzites unit defined by angular grains, high overall feldspar (Fk: alkalifeldspar; Fp: plagioclase) proportions and abundant detrital matrix. L) Abundant calcite cement precipitation characteristic of the uppermost sample of the Ubaghetta section.

Fig. 5. Modal framework composition of the analysed samples from the Monte Bignone Sandstones and interpreted provenance discrimination fields (QtFL plot after Dickinson et al., 1983; QmFLt plot Dickinson & Suczek, 1979). Note the up-section trend from quartzose sandstones to litharenites in the Lower Quartzites unit and the subsequent shift towards a quartzolithic-feldspathic composition characteristic of the Upper Quartzites unit.

Fig. 6. Stratigraphic changes of modal composition. QFLt plot on the left and detailed lithic clast components (Qp: polycrystalline quartz, Lm/p: metamorphic/plutonic fragment, Lv: volcanic fragment, Lsed: sedimentary fragment, Ldolo: dolostone fragment and LCe: calcareous lithithic fragment), on the right. A) Samples UR_01 to UR_03 from a ca. 30 m thick section through the Upper Quartzites unit in the more distal domain (locality Ubaghetta). B) Samples PA_01 to PA27 from a 40 m thick section through the Lower Quartzites unit in the more proximal domain (locality Capo Croce). See Fig. 1 for locations and Fig. 2C-D for samples stratigraphic positions. Note how the QFLt plot for the Lower Quartzites unit illustrates the systematic up-section increase in lithic grains at the expense of total quartz, a trend which is contrasted by the overall stratigraphic pattern recorded in the Upper Quartzites unit.

Fig. 7. Representative cathodoluminescence images of analysed detrital zircons with approximate ablation spot location. Yellow scale bars are 100 microns long.

Fig. 8. A) Detrital age spectra (probability density plot) of the Monte Bignone Sandstones for the time interval 0-3500 Ma (bin width: 50 Ma). B) Detrital age distribution in the time interval 200-1200 Ma. C) Qualitative comparison of detrital zircon age data of the analysed samples with that from other siliciclastic members of the WLF (Bordighera Sandstones and San Bartolomeo Formation (SBF); Mueller et al., 2018). Geological time-scale according to the International Commission on Stratigraphy.

Fig. 9. A) Idealized compositional evolutions illustrating the unroofing of contrasting source terranes as documented in the detrital modes of the siliciclastic members of the WLF. This model (A) is derived from the comparison of the compositional stratigraphic evolution (arrow indicates younging direction) of the two main siliciclastic successions of the Western Ligurian Flysch Units (B and C). B) Compositional trends of the first-cycle Bordighera Sandstones and the underlying basal complex (Mueller et al. 2018). C) Compositional trends of the polycyclic Monte Bignone Sandstones (this study). Provenance discrimination fields after Dickinson et al. (1983).

Fig. 10. Cumulative distribution functions of detrital zircon ages from siliciclastic successions derived from the Southern European Variscan basement blocks from this study (MBS) and from candidates from published literature (Money Unit: Manzotti et al. 2015; Zone Houillère and Pinerolo Unit: Manzotti et al. 2016) for the time span from 0 to 3500 Ma.

Fig. 11. Non-metric multidimensional scaling (MDS) plot of compiled detrital zircon age datasets (29 datasets; 2955 ages) of selected pre- and syn-orogenic siliciclastic successions deposited in the context of the Alpine Cycle. The compilation of detrital ages is reported in the supplementary data file. Note the distinct cluster of U-Pb detrital age spectra of palaeo-Europe-derived successions highlighted by the green outline in the left.

Figure 1

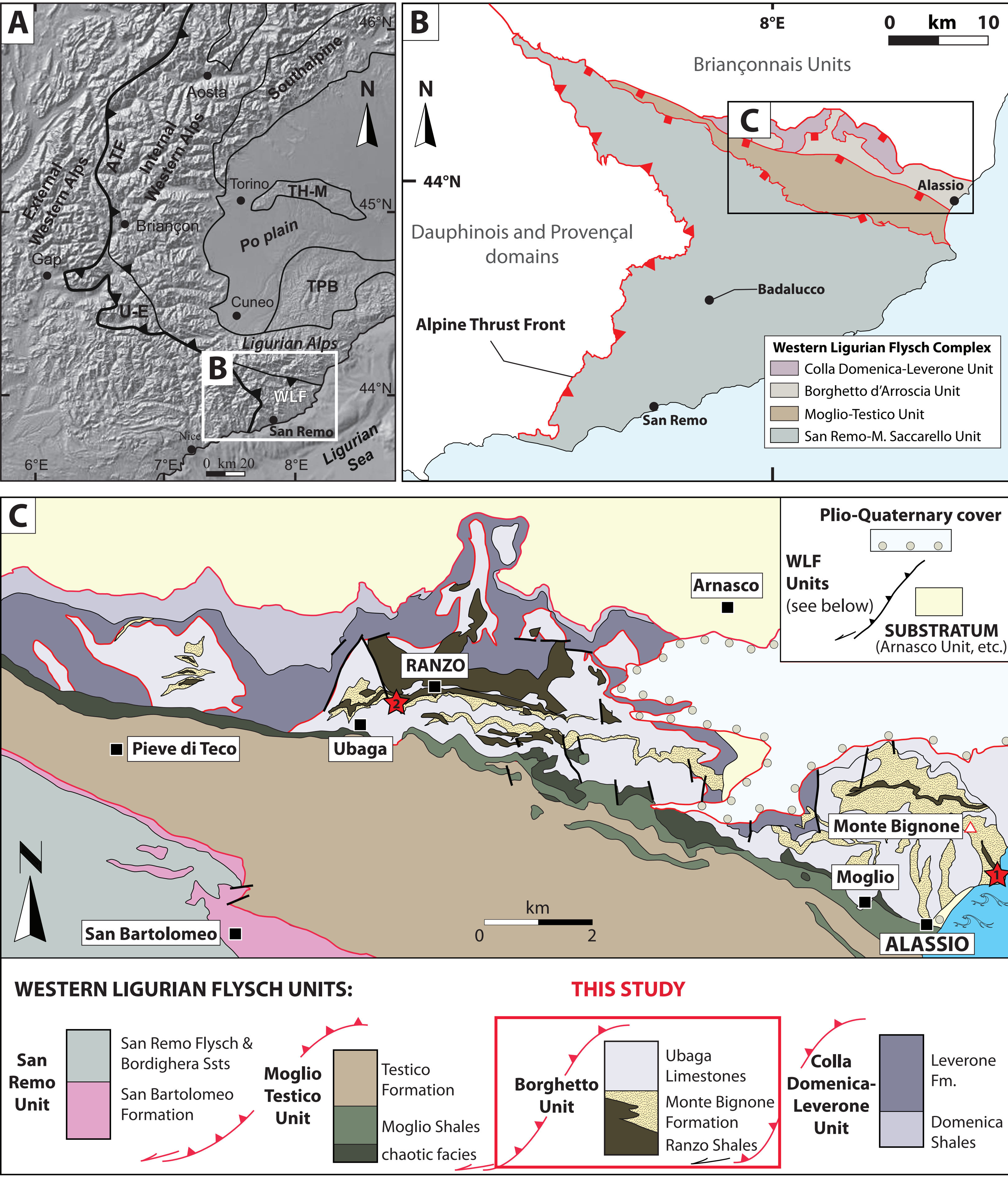
A
46°N
Aosta
Southalpine
N
ATF
Internal Western Alps
External Western Alps
Torino
TH-M
45°N
Briançon
Po plain
Gap
TPB
Cuneo
U-E
Ligurian Alps
B
WLF
44°N
San Remo
Nice
Ligurian Sea
6°E
7°E
0 km 20
8°E
B
8°E
0 km 10
Briançonnais Units
N
C
44°N
Alassio
Dauphinois and Provençal domains
Badalucco
Alpine Thrust Front
Western Ligurian Flysch Complex
Colla Domenica-Leverone Unit
Borghetto d'Arroscia Unit
Moglio-Testico Unit
San Remo-M. Saccarello Unit
San Remo
C
Plio-Quaternary cover
Arnasco
WLF Units (see below)
SUBSTRATUM (Arnasco Unit, etc.)
RANZO
Pieve di Teco
Ubaga
Monte Bignone
Moglio
San Bartolomeo
km
0
2
ALASSIO
WESTERN LIGURIAN FLYSCH UNITS:
THIS STUDY
San Remo Unit
San Remo Flysch & Bordighera Ssts
San Bartolomeo Formation
Moglio Testico Unit
Testico Formation
Moglio Shales
chaotic facies
Borghetto Unit
Ubaga Limestones
Monte Bignone Formation
Ranzo Shales
Colla Domenica-Leverone Unit
Leverone Fm.
Domenica Shales

Figure 2

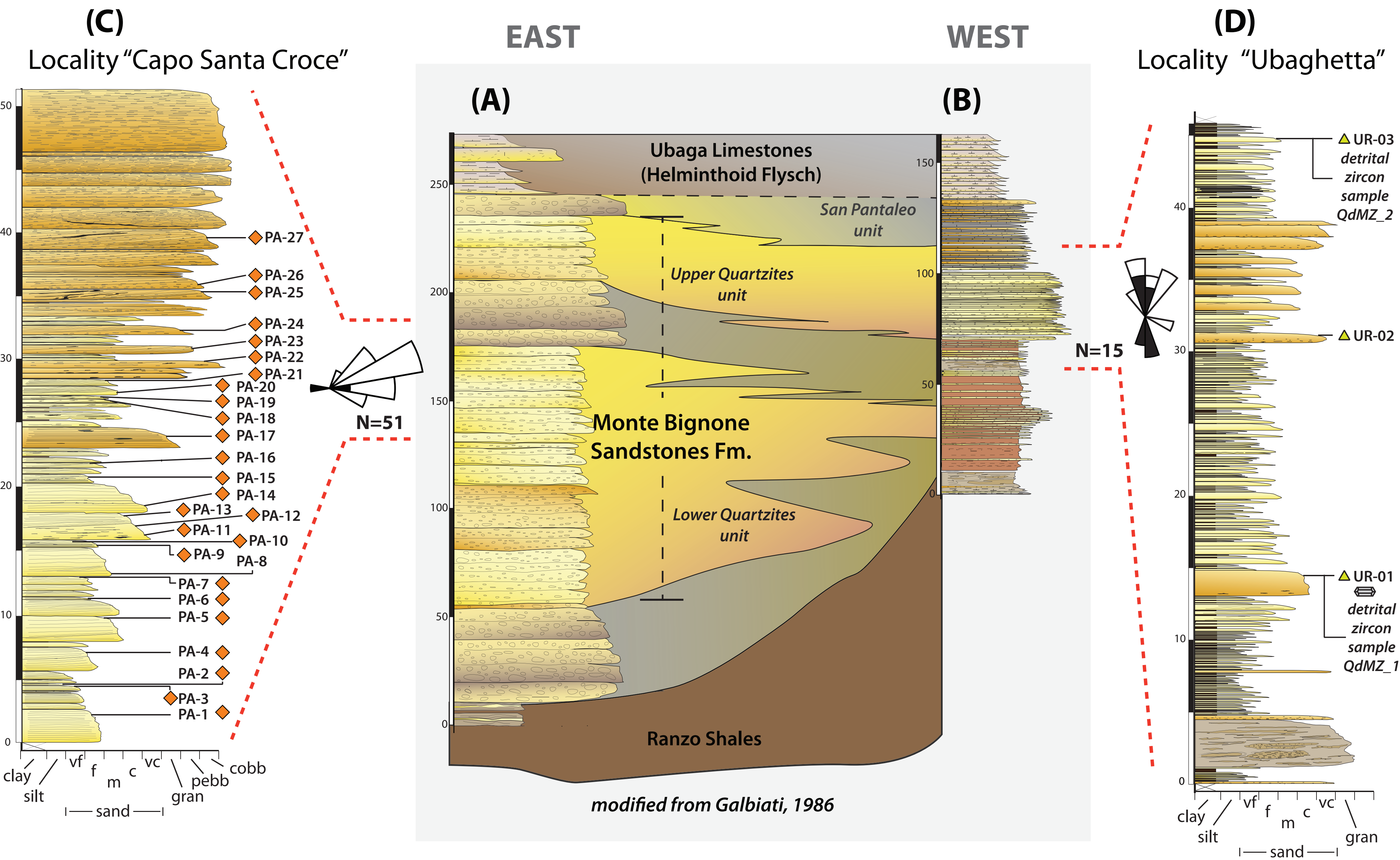

(C)
Locality "Capo Santa Croce"
EAST
WEST
(D)
Locality "Ubaghetta"
(A)
(B)
Ubaga Limestones
(Helminthoid Flysch)
San Pantaleo unit
Upper Quartzites unit
Monte Bignone Sandstones Fm.
Lower Quartzites unit
Ranzo Shales
modified from Galbiati, 1986
N=51
N=15
PA-27
PA-26
PA-25
PA-24
PA-23
PA-22
PA-21
PA-20
PA-19
PA-18
PA-17
PA-16
PA-15
PA-14
PA-13
PA-12
PA-11
PA-10
PA-9
PA-8
PA-7
PA-6
PA-5
PA-4
PA-2
PA-3
PA-1
UR-03
detrital zircon sample QdMZ_2
UR-02
UR-01
detrital zircon sample QdMZ_1
clay
silt
vf
f
m
c
vc
sand
gran
pebb
cobb

Figure 3

Figure 4

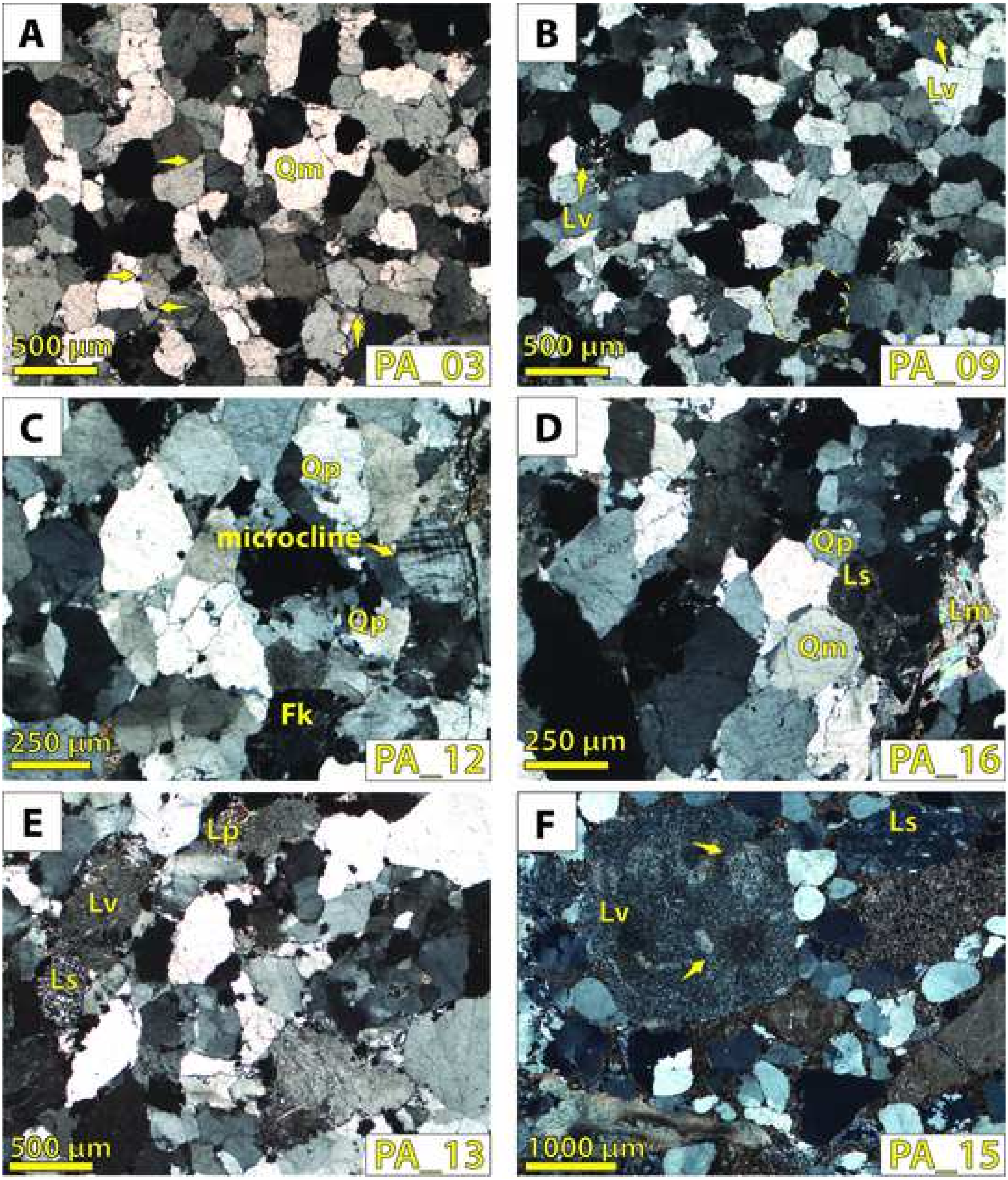
A
Qm
500 µm
PA_03
B
Lv
Lv
500 µm
PA_09
C
Qp
microcline
Qp
Fk
250 µm
PA_12
D
Qp
Ls
Lm
Qm
250 µm
PA_16
E
Lp
Lv
Ls
500 µm
PA_13
F
Ls
Lv
1000 µm
PA_15

Figure 4

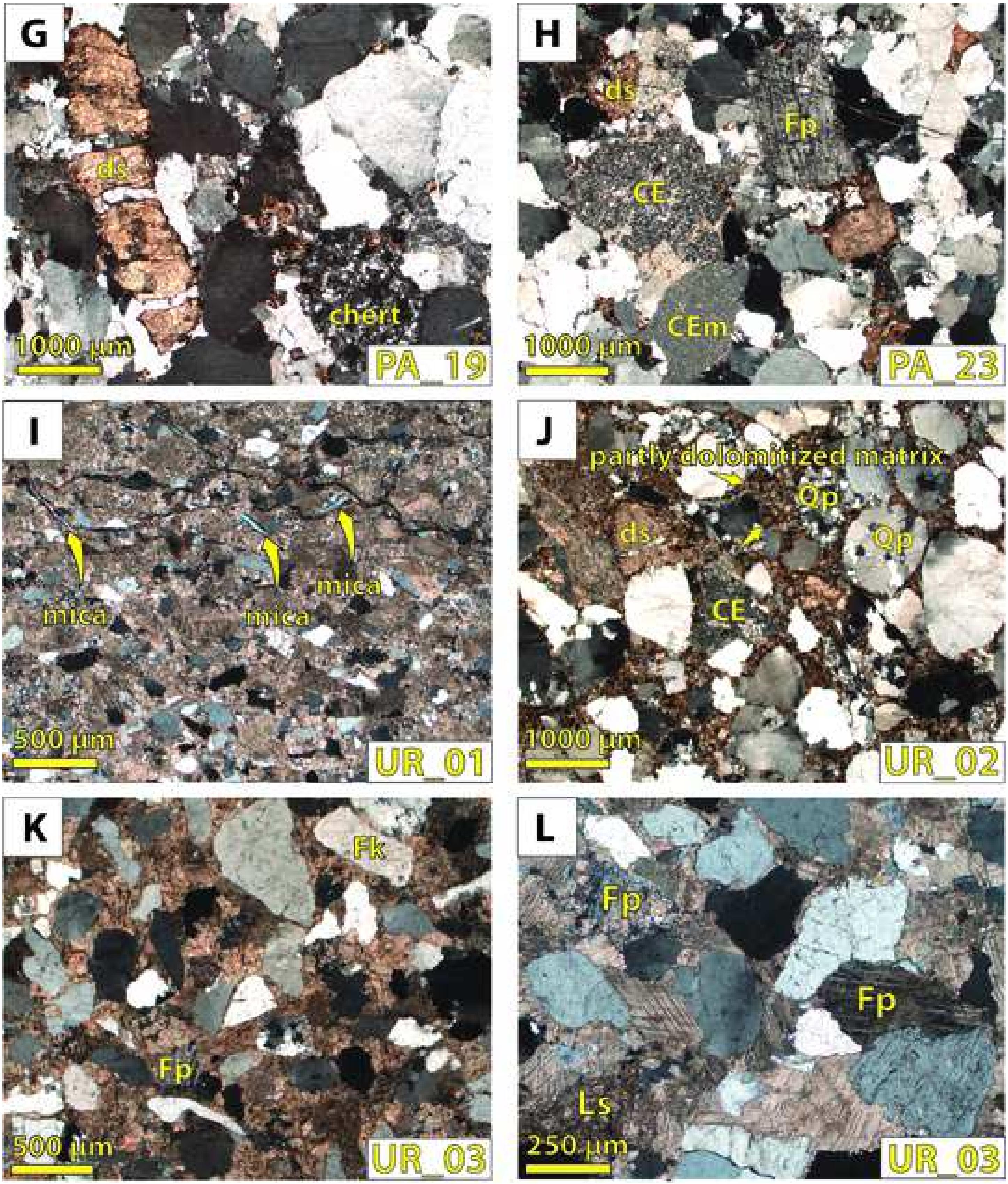
G
ds
chert
1000 µm
PA_19
H
ds
Fp
CE
CEm
1000 µm
PA_23
I
mica
mica
mica
500 µm
UR_01
J
partly dolomitized matrix
Qp
Qp
ds
CE
1000 µm
UR_02
K
Fk
Fp
500 µm
UR_03
L
Fp
Fp
Ls
250 µm
UR_03

Figure 5

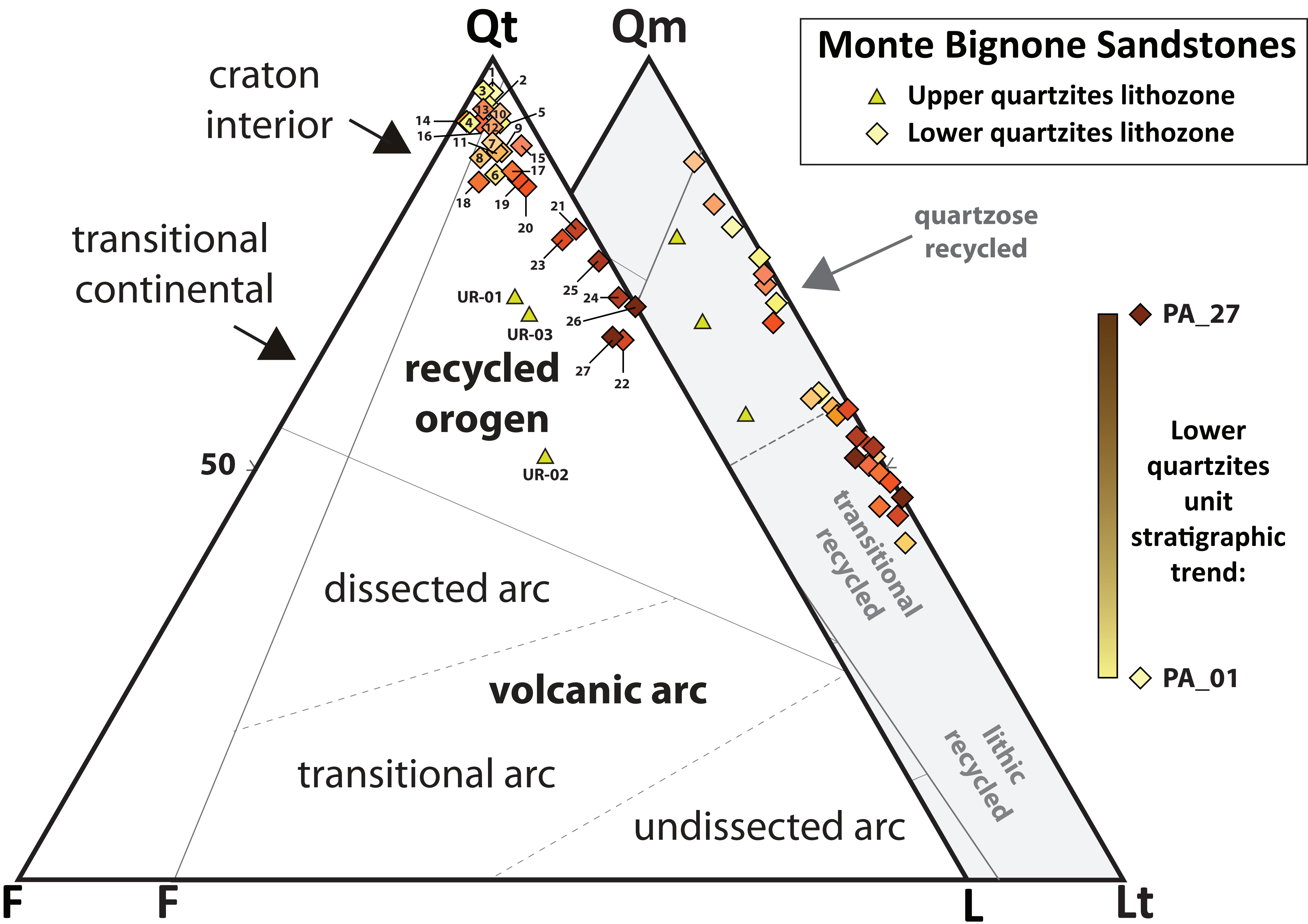

Qt
Qm
Monte Bignone Sandstones
Upper quartzites lithozone
Lower quartzites lithozone
craton
interior
transitional
continental
recycled
orogen
quartzose
recycled
transitional
recycled
lithic
recycled
dissected arc
volcanic arc
transitional arc
undissected arc
50
UR-01
UR-03
UR-02
PA_27
Lower
quartzites
unit
stratigraphic
trend:
PA_01
F
F
L
Lt

Figure 6

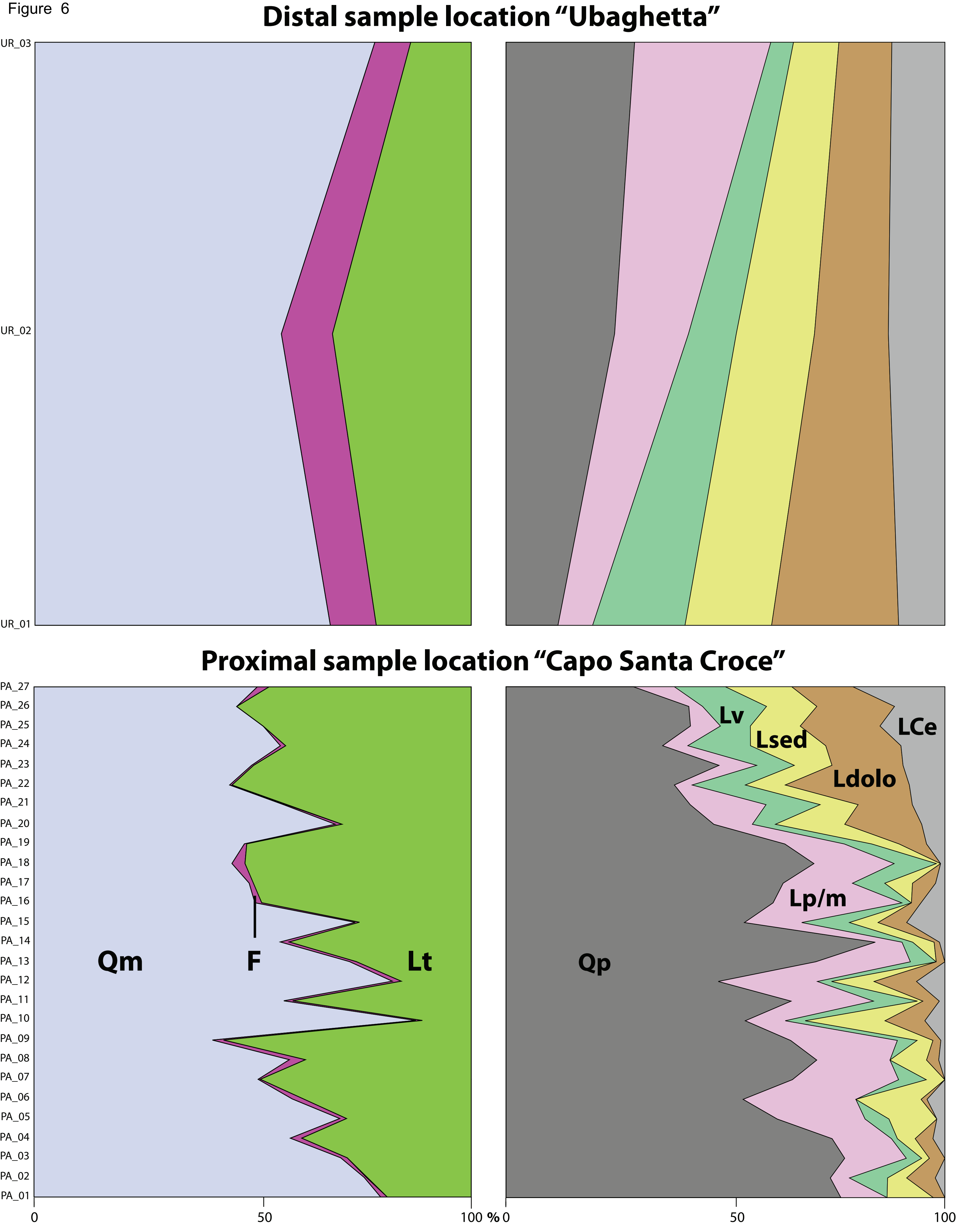

Distal sample location "Ubaghetta"
UR_03
UR_02
UR_01
Proximal sample location "Capo Santa Croce"
PA_27
PA_26
PA_25
PA_24
PA_23
PA_22
PA_21
PA_20
PA_19
PA_18
PA_17
PA_16
PA_15
PA_14
PA_13
PA_12
PA_11
PA_10
PA_09
PA_08
PA_07
PA_06
PA_05
PA_04
PA_03
PA_02
PA_01
Qm
F
Lt
Qp
Lv
Lsed
LCe
Ldolo
Lp/m
0
50
100 %
0
50
100

Figure 7

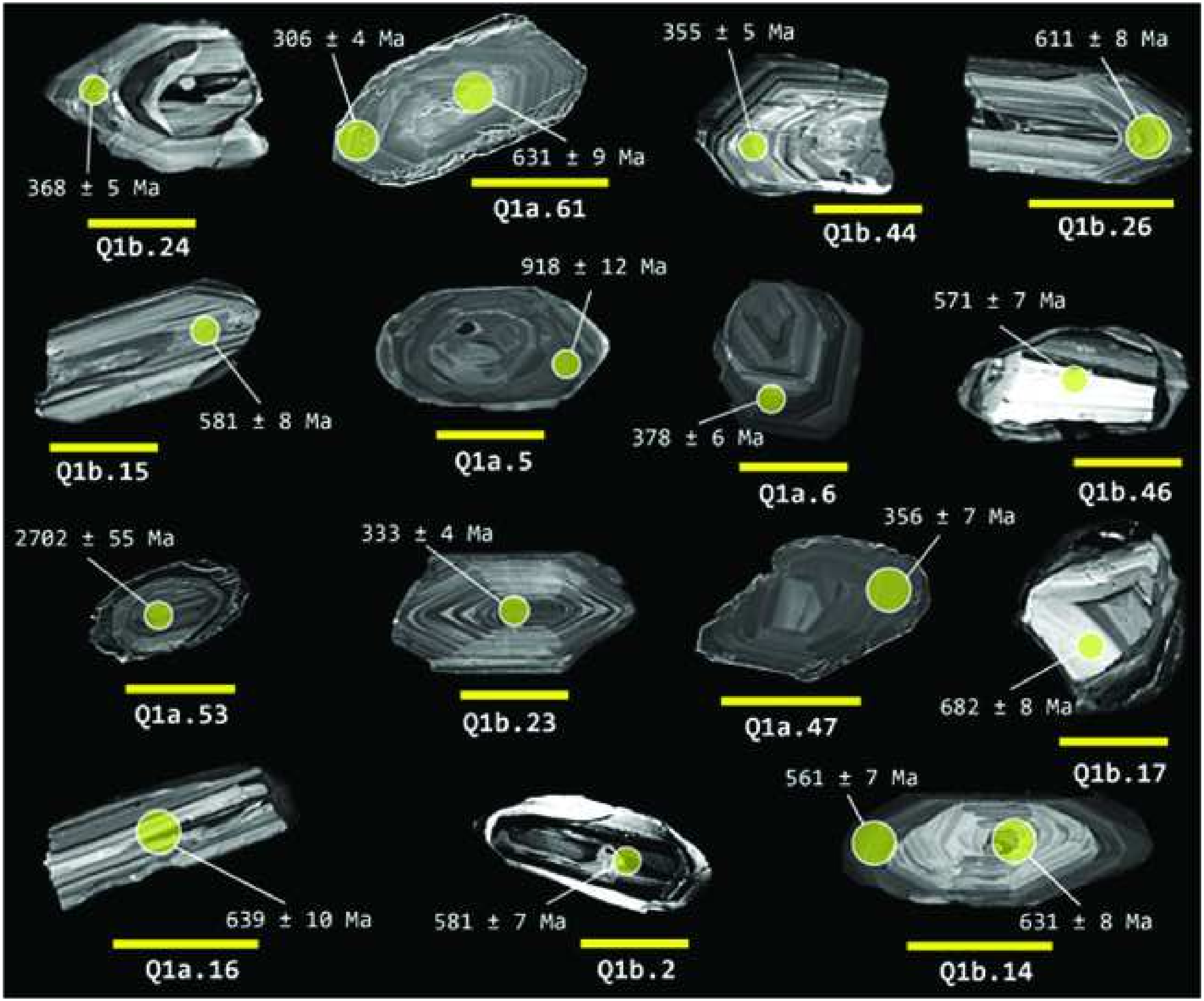

368 ± 5 Ma
Q1b.24
306 ± 4 Ma
631 ± 9 Ma
Q1a.61
355 ± 5 Ma
Q1b.44
611 ± 8 Ma
Q1b.26
581 ± 8 Ma
Q1b.15
918 ± 12 Ma
Q1a.5
378 ± 6 Ma
Q1a.6
571 ± 7 Ma
Q1b.46
2702 ± 55 Ma
Q1a.53
333 ± 4 Ma
Q1b.23
356 ± 7 Ma
Q1a.47
682 ± 8 Ma
Q1b.17
639 ± 10 Ma
Q1a.16
581 ± 7 Ma
Q1b.2
561 ± 7 Ma
631 ± 8 Ma
Q1b.14

Figure 8

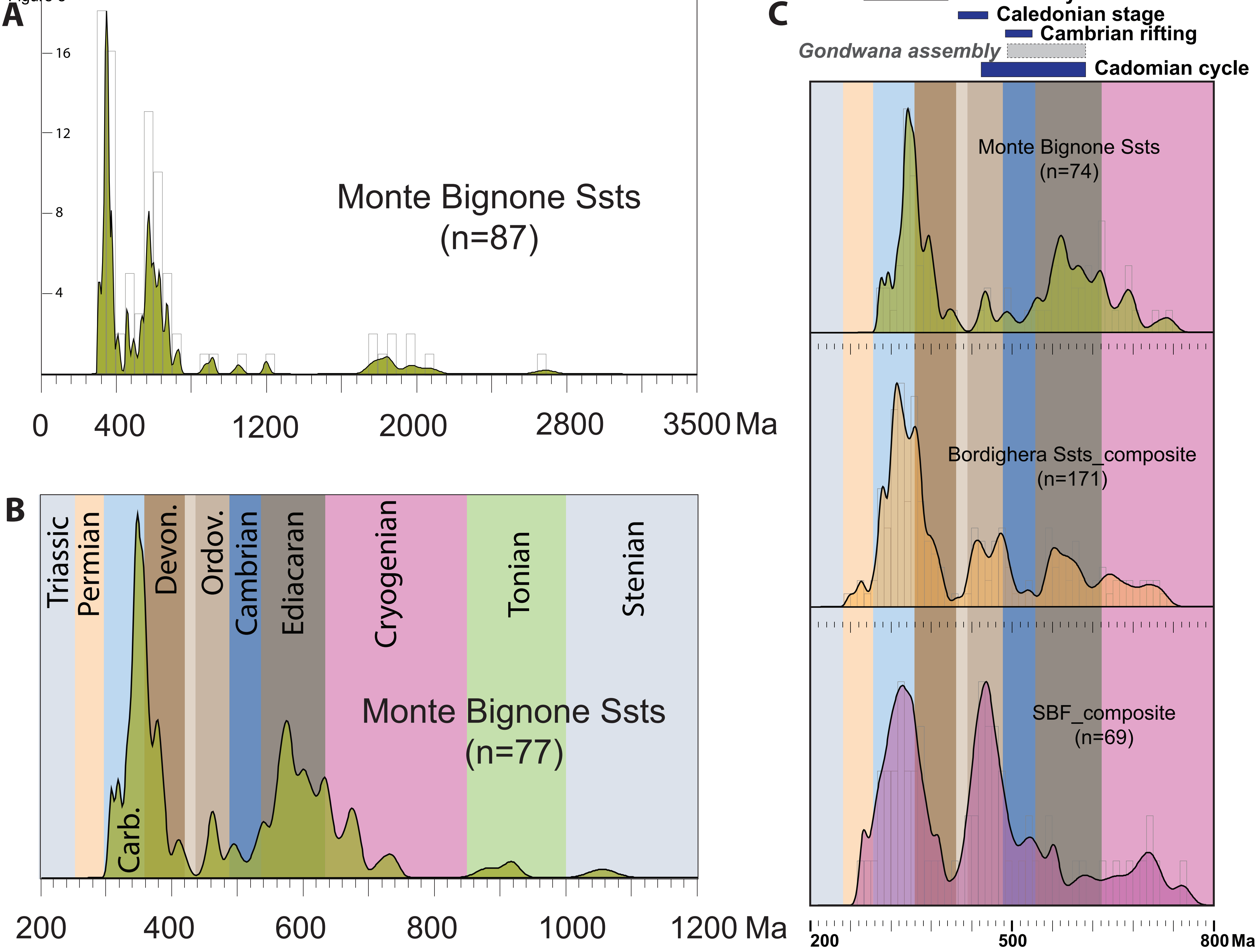

A
16
12
8
4
Monte Bignone Ssts
(n=87)
0
400
1200
2000
2800
3500
Ma
B
Triassic
Permian
Carb.
Devon.
Ordov.
Cambrian
Ediacaran
Cryogenian
Tonian
Stenian
Monte Bignone Ssts
(n=77)
200
400
600
800
1000
1200 Ma
C
Variscan cycle
Caledonian stage
Cambrian rifting
Gondwana assembly
Cadomian cycle
Monte Bignone Ssts
(n=74)
Bordighera Ssts_composite
(n=171)
SBF_composite
(n=69)
200
500
800
Ma

Figure 9

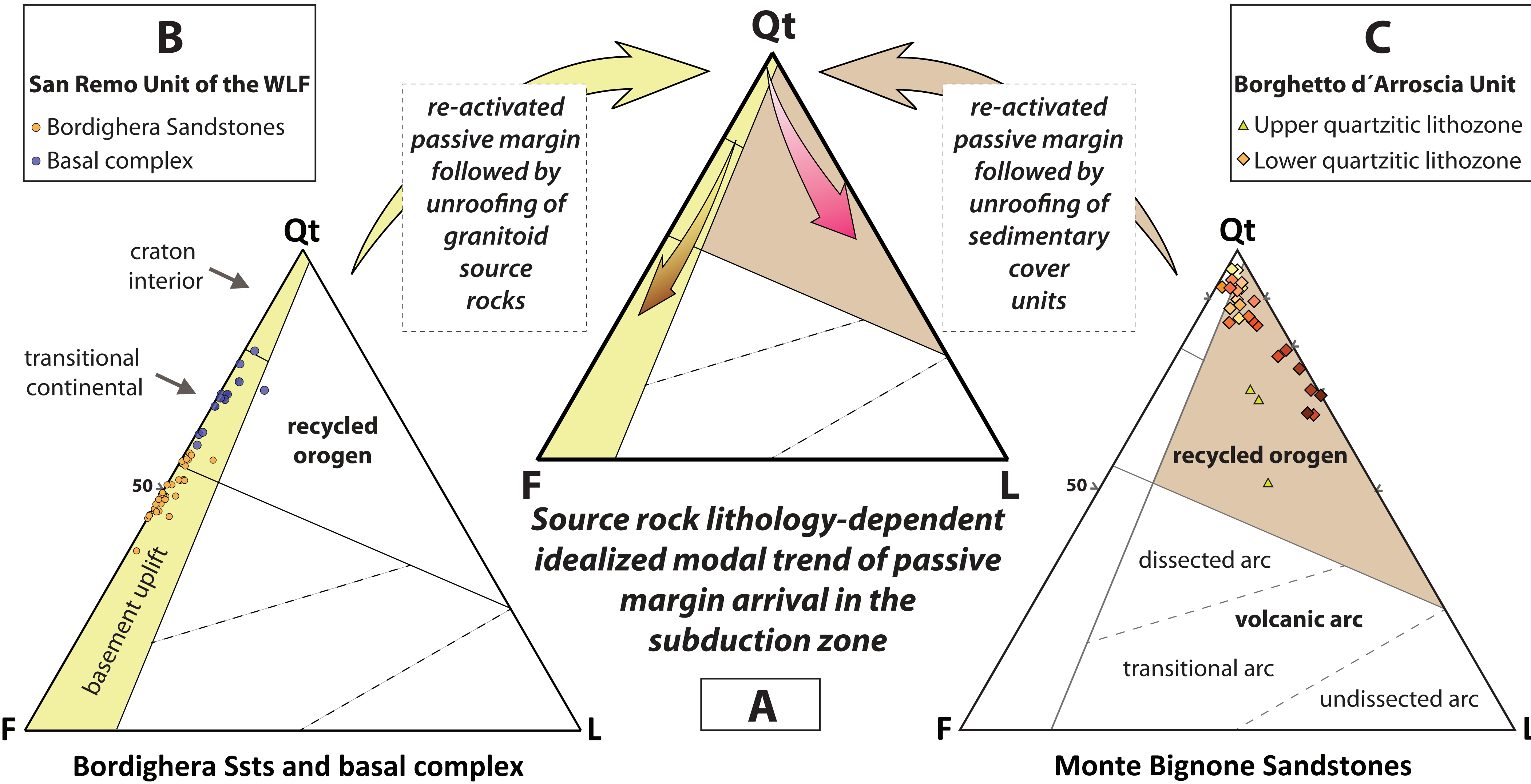

B
San Remo Unit of the WLF
Bordighera Sandstones
Basal complex
Qt
craton interior
transitional continental
recycled orogen
50
basement uplift
F
L
Bordighera Ssts and basal complex
re-activated passive margin followed by unroofing of granitoid source rocks
Qt
F
L
re-activated passive margin followed by unroofing of sedimentary cover units
Source rock lithology-dependent idealized modal trend of passive margin arrival in the subduction zone
A
C
Borghetto d´Arroscia Unit
Upper quartzitic lithozone
Lower quartzitic lithozone
Qt
50
recycled orogen
dissected arc
volcanic arc
transitional arc
undissected arc
F
L
Monte Bignone Sandstones

Figure 10

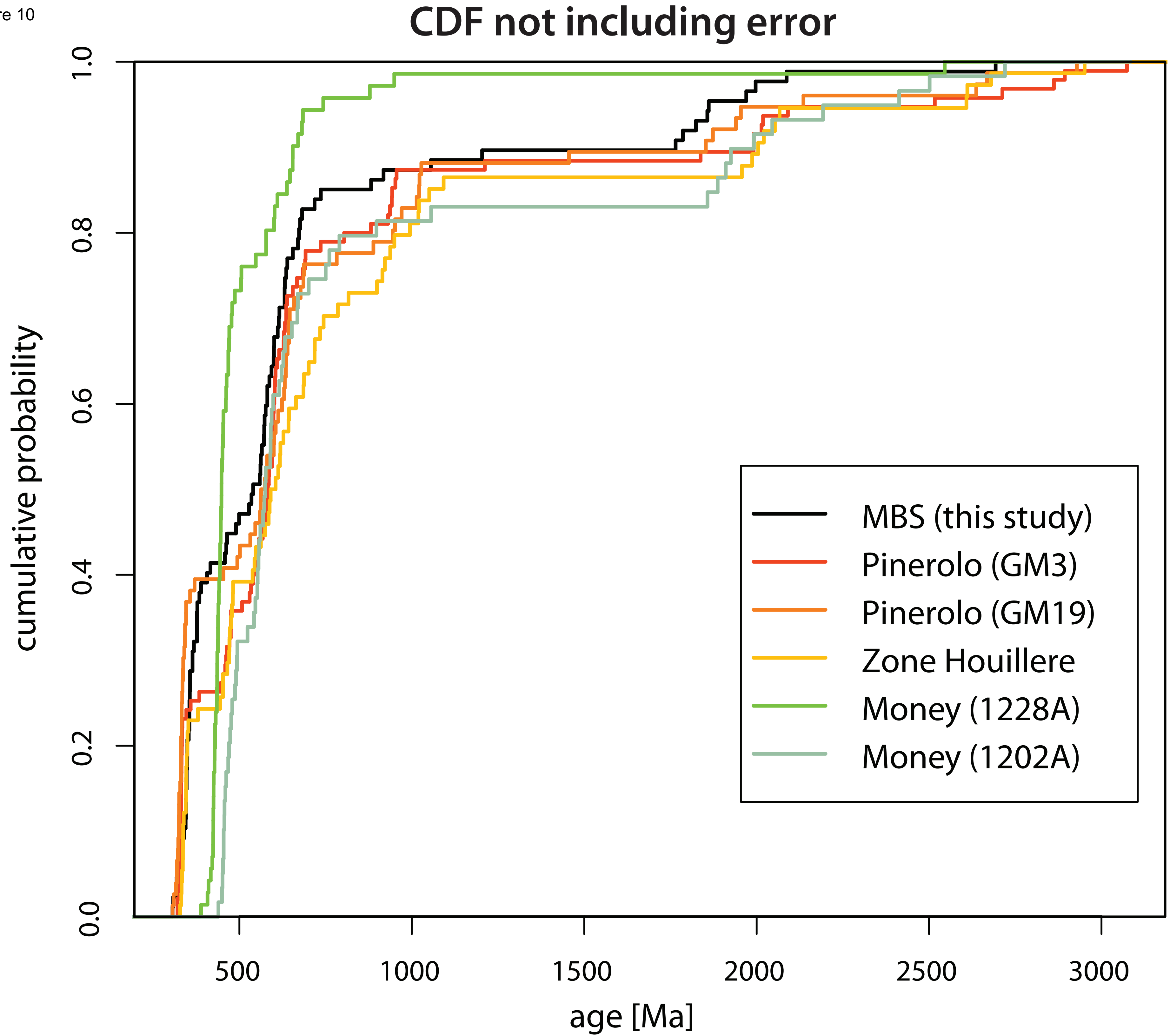
CDF not including error
cumulative probability
0.0
0.2
0.4
0.6
0.8
1.0
500
1000
1500
2000
2500
3000
age [Ma]
MBS (this study)
Pinerolo (GM3)
Pinerolo (GM19)
Zone Houillere
Money (1228A)
Money (1202A)

Figure 11

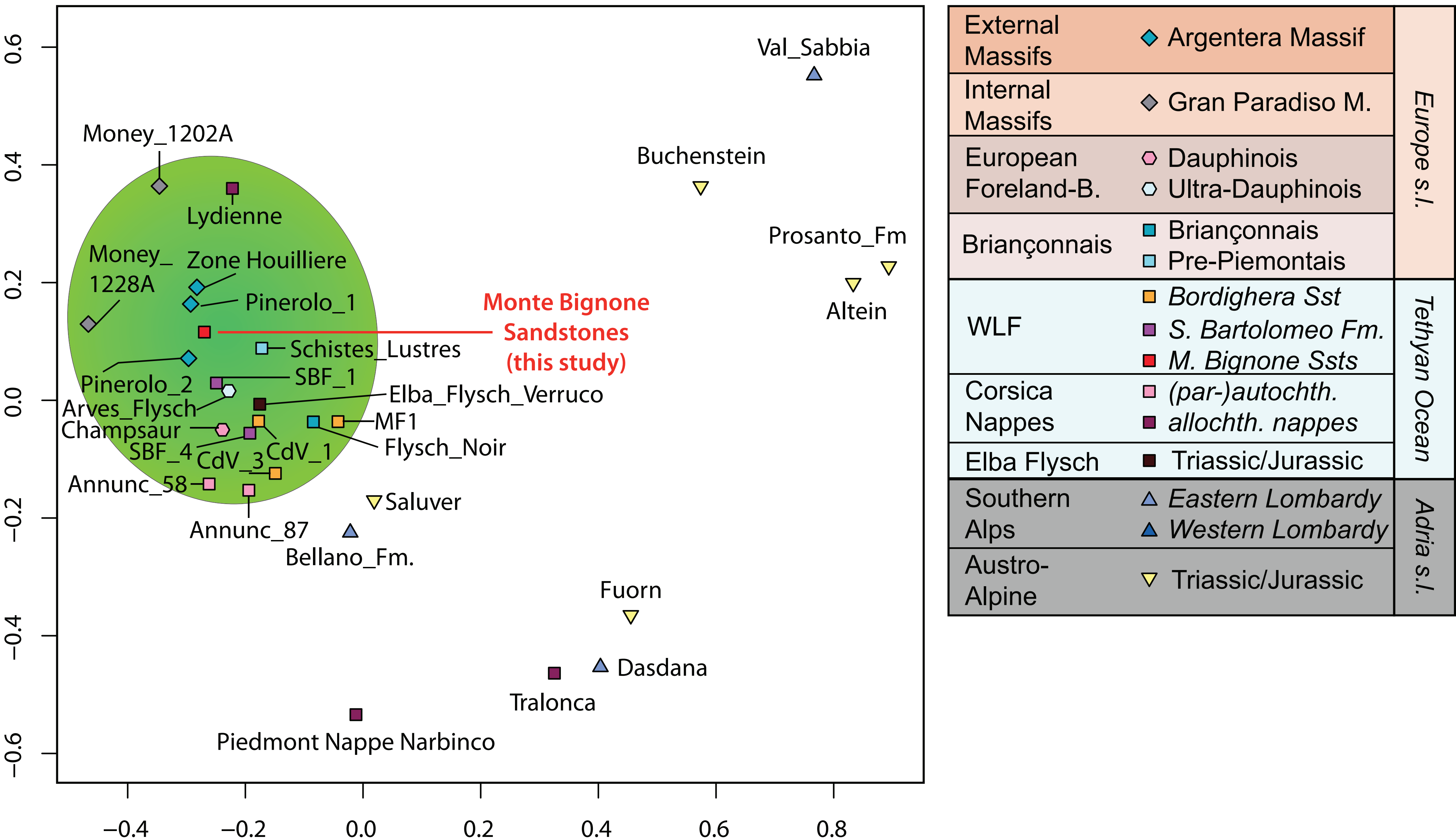

0.6
0.4
0.2
0.0
−0.2
−0.4
−0.6
−0.4
−0.2
0.0
0.2
0.4
0.6
0.8
Val_Sabbia
Money_1202A
Buchenstein
Lydienne
Prosanto_Fm
Money_
1228A
Zone Houilliere
Pinerolo_1
Altein
Monte Bignone
Sandstones
(this study)
Schistes_Lustres
SBF_1
Pinerolo_2
Elba_Flysch_Verruco
Arves_Flysch
MF1
Champsaur
SBF_4
CdV_3
CdV_1
Flysch_Noir
Annunc_58
Saluver
Annunc_87
Bellano_Fm.
Fuorn
Dasdana
Tralonca
Piedmont Nappe Narbinco
External Massifs
Argentera Massif
Internal Massifs
Gran Paradiso M.
European Foreland-B.
Dauphinois
Ultra-Dauphinois
Briançonnais
Briançonnais
Pre-Piemontais
WLF
Bordighera Sst
S. Bartolomeo Fm.
M. Bignone Ssts
Corsica Nappes
(par-)autochth.
allochth. nappes
Elba Flysch
Triassic/Jurassic
Southern Alps
Eastern Lombardy
Western Lombardy
Austro-Alpine
Triassic/Jurassic
Europe s.l.
Tethyan Ocean
Adria s.l.